Journal of Sustainable Cement-Based Materials

ISSN: (Print) (Online) Journal homepage: www.tandfonline.com/journals/tscm20

Development of novel ultra-high-performance lightweight concrete modified with dehydrated cement powder and aerogel

Ahmed Ali A. Shohan, Osama Zaid, Mohamed M. Arbili, Saleh Hamed Alsulamy & Wafeek Mohamed Ibrahim

To cite this article: Ahmed Ali A. Shohan, Osama Zaid, Mohamed M. Arbili, Saleh Hamed Alsulamy & Wafeek Mohamed Ibrahim (2024) Development of novel ultra-high-performance lightweight concrete modified with dehydrated cement powder and aerogel, Journal of Sustainable Cement-Based Materials, 13:3, 351-374, DOI: 10.1080/21650373.2023.2278134

To link to this article: https://doi.org/10.1080/21650373.2023.2278134

Published online: 05 Nov 2023.

Journal of Sustainable Cement-Based Materials, 2024
Vol. 13, No. 3, 351–374, http://dx.doi.org/10.1080/21650373.2023.2278134

Development of novel ultra-high-performance lightweight concrete modified with dehydrated cement powder and aerogel

Ahmed Ali A. Shohan[a], Osama Zaid[b]*, Mohamed M. Arbili[c], Saleh Hamed Alsulamy[d] and Wafeek Mohamed Ibrahim[a]

[a]*Architecture and Planning Department, Faculty of Engineering, King Khalid University (KKU), Abha, Saudi Arabia;* [b]*Department of Civil Engineering, Swedish College of Engineering and Technology, Wah Cantt, Pakistan;* [c]*Department of Technical Civil Engineering, Erbil Technical Engineering College, Erbil Polytechnic University, Erbil, Iraq;* [d]*Department of Architecture and Planning, College of Engineering, King Khalid University, Abha, Saudi Arabia*

Abstract. Currently, researchers emphasize creating eco-friendly, ultra-high-performance lightweight concrete (UHPLC) due to the extensive cement demand of ultra-high-performance concrete. This study aimed to develop such UHPLC by incorporating dehydrated cement powder (DCP) and aerogel (AG) at varying levels (5-25%) alongside double-hooked end steel fibers (DHE-SFs). Objectives were to enhance strength, durability, density, and thermal/acoustic properties. Results revealed reduced flowability with higher DCP and AG content. 5%, 10%, and 15% DCP and AG improved compressive strength (17.3%) *via* better packing and bond formation. Density decreased up to 8.3% with more DCP and AG. Modified mixtures resisted sulfate attack and exhibited increased compressive strength retention. Shrinkage reduced to 958 μ with more DCP and AG, notably in M6-DCP25-AG25. Thermal stability improved with only 75.4% mass loss at 1000 °C, while thermal conductivity decreased to 0.274 W/m·°C. Sound absorption and pore volume increased in modified mixes. X-ray diffraction analysis showed higher crystalline phases with increased DCP and AG.

Keywords: thermal analysis; acoustics; pore structure; shrinkage; porosity

1. Introduction

In recent years, due to its exceptional engineering properties, there has been a notable shift in the engineering and research community's focus from conventional concrete to ultra-high-performance concrete (UHPC) [1]. UHPC offers many advantages over traditional concrete, including significantly higher compressive and tensile strengths, improved durability, enhanced resistance to corrosion and impact, and the ability to create lighter and more slender structures [2,3]. These properties make UHPC an attractive choice for various applications, including bridges, high-rise buildings, and infrastructure projects [4]. However, one major challenge associated with UHPC is its high consumption of ordinary Portland cement (OPC), the key binding agent in concrete [5]. OPC production is a major source of carbon dioxide (CO_2) emissions, accounting for a significant portion of global greenhouse gas emissions [6]. Manufacturing OPC involves heating limestone and other materials to high temperatures, which requires substantial energy and releases CO_2 as a byproduct. Consequently, using OPC in UHPC can contribute to the construction industry's carbon footprint and hinder efforts to reduce CO_2 emissions [7]. The United States emitted approximately 4.6 billion metric tons of CO_2 in 2021, with the construction industry contributing significantly to these emissions. The United Kingdom emitted around 361 million metric tons of CO_2, with the construction sector playing a role in the overall emissions. China, as the world's largest emitter, released approximately 10.5 billion metric tons of CO_2 in 2021, and the construction industry in China contributes significantly to these emissions. India emitted around 2.6 billion metric tons of CO_2, including contributions from the construction sector [8]. European countries, as a whole, emitted approximately 3.4 billion metric tons of CO_2 in 2021, with the construction industry's emissions encompassing the use of OPC in UHPC [9,10].

Dehydrated cement powder (DCP) has emerged as a potential solution to reduce the usage of OPC in the development of UHPC [11]. DCP is a finely ground powder obtained by dehydrating and pulverizing cementitious materials, such as OPC, at high temperatures. When used as a partial substitute for OPC in UHPC mixtures, DCP offers several benefits. Incorporating DCP in UHPC helps lower the overall OPC content, reducing the environmental influence of OPC manufacturing and its CO_2 emissions [12]. DCP promotes the formation of additional hydration products [13]. These products fill the gaps between OPC particles, enhancing the interfacial transition zone between cement paste and aggregates. This improved interfacial bond leads to enhanced load transfer and reduced vulnerability to cracking, thereby increasing the overall structural integrity of the UHPC [9, 14]. DCP particles are finer than OPC particles, which allows for a more densely packed matrix in the UHPC. This enhanced particle packing improves mechanical properties, including higher

*Corresponding author. Email: Osama.zaid@scetwah.edu.pk

compressive and flexural strengths. DCP also contributes to increased density and reduced porosity in the UHPC, leading to improved durability against chemical attacks, freezing-thawing cycles, and abrasion. Using DCP in UHPC can contribute to improved workability and reduced water demand. Due to the finer particle size, DCP particles have a larger surface area, allowing for better particle dispersion and lubrication. This results in improved flowability during mixing and placement, facilitating the casting of intricate shapes and reducing the need for excessive water content. The lower water-to-cement ratio achieved through DCP utilization helps enhance the strength and durability of the UHPC.

There is a growing inclination and requirement for energy conservation, minimizing the burden on material resources, and mitigating pollution [15,16]. The focus on energy-efficient buildings with minimal adverse environmental impact has gained significant traction within this context [17]. Zero-emission buildings are a potential pathway toward a sustainable future [18]. Because of the conventional concrete's high thermal conductivity (1.7–2.5 W/(m·K) and non-efficient in energy preservation, the researchers have redirected their attention from conventional heavyweight concrete to ultra-high-performance lightweight concrete (UHPLC) [19,20]. The construction industry's need for improved thermal insulation and energy efficiency primarily drives this shift. While conventional concrete has high thermal conductivity, UHPLC offers excellent heat preservation and superior thermal insulation properties [21]. UHPLC is designed to have a significantly reduced density compared to normal-weight concrete [22,23], achieved by incorporating lightweight aggregates or air-entraining agents. This lower density results in improved heat preservation capabilities, making UHPLC an attractive choice for applications that require enhanced energy efficiency [24]. By minimizing heat transfer through the building envelope, UHPLC helps reduce heating and cooling demands, resulting in lower energy consumption and reduced environmental impact [25]. The excellent thermal insulation provided by UHPLC offers additional benefits, such as enhanced occupant comfort and reduced reliance on mechanical heating and cooling systems [26,27]. Structures constructed with UHPLC can maintain more stable indoor temperatures, reducing temperature fluctuations and creating a more comfortable living or working environment [28,29]. Moreover, the reduced energy demand for temperature control contributes to lower greenhouse gas emissions and promotes sustainability in the built environment [18, 30]. UHPLC retains the outstanding building and mechanical characteristics associated with UHPC [31–33]. It offers exceptional strength, durability, and resistance to various external factors such as corrosion, impact, and fire. These properties make UHPLC a highly versatile material for various applications, including high-rise buildings, bridges, and infrastructure projects.

Aerogel has emerged as a promising material for enhancing the properties of UHPLC by partially substituting it for fine aggregates [34]. AG is an ultralight, porous material derived from a gel, in which the liquid component has been replaced with gas. The introduction of AG in UHPLC has a history rooted in achieving better thermal insulation properties while maintaining or improving the strength and durability of the concrete. Aerogel offers several benefits when used as a partial replacement for fine aggregates. AG has extremely low thermal conductivity, making it an excellent insulator [35]. Incorporating AG into UHPLC helps to enhance its heat preservation capabilities, resulting in improved energy efficiency and reduced heat transfer through the structure. This makes it well-suited for applications with critical thermal insulation, such as buildings and infrastructure, where energy savings and occupant comfort are paramount [36]. AG possesses remarkable mechanical properties, including high compressive strength and excellent load-bearing capacity [37]. By introducing AG into UHPLC, it is possible to maintain or even improve the strength and durability properties of the concrete [38]. This allows lightweight structures with enhanced structural integrity and resistance to external factors such as corrosion, impact, and fire [39]. AG is also highly compatible with UHPLC. Its lightweight nature ensures that the overall density of the concrete is reduced, resulting in a lighter structure that can offer further advantages such as reduced dead load, improved seismic performance, and easier handling during construction.

The demand for architecturally complex structures, long-span bridges, tunnels, and high-rise structures leads to significantly high-cost and heavy-weight structures. The above studies suggest to commercial development of a sustainable, eco-friendly, and low-energy concrete with excellent engineering properties for structural applications; it is essential to partially replace the OPC and fine aggregate with sustainable recycled cementitious material and suitable lightweight material to develop a low-carbon UHPLC, which will be widely accepted by the construction sector and utilized in different structural applications due to its improved properties under different harsh conditions.

Previous research indicates that while numerous attempts have been made to produce eco-friendly UHPC or lightweight UHPC, there has been a noticeable gap in developing eco-friendly, UHPLC enriched with dehydrated cement powder and aerogel. This study aims to bridge this gap by presenting an innovative approach to making low-carbon, UHPLC. This is achieved by substituting ordinary Portland cement with dehydrated cement powder and replacing fine aggregate with aerogel in varying proportions (5%, 10%, 15%, 20%, and 25% by weight). The evaluation process encompassed a range of tests and analyses, including flowability assessment, examination of physical properties like compressive, flexural, and bonding strength, as well as density and ultrasonic pulse velocity. Harsh durability attributes were studied, such as resistance to sulfate attack, shrinkage, and thermal properties. Functional characteristics, namely thermal conductivity, and acoustics, were evaluated, and microstructural investigations were conducted, focusing

on pore diameter and x-ray diffraction. All mix compositions incorporated two percent (by binder's weight) of double-hooked end steel fibers (DHE-SFs). This research represents a pioneering stride towards the realization of energy-efficient, high-performance construction materials. By leveraging the notable thermal insulation and mechanical strength of aerogel, it provides a pathway for structural engineers and researchers to develop enhanced and novel UHPLC.

2. Raw materials and design of concrete samples

The current research used 53-grade type-I locally available OPC per ASTM C150 [28]. The silica fume (SF) utilized in the current study showcased remarkable fineness, boasting a specific surface area of 19.1 m^2/g. Dehydrated Cement Powder is typically developed from recycled cementitious waste construction materials (RCWCM). The recycling process is displayed in Figure 1. RCWCM can be sourced from various outlets, including abandoned concrete, where the fine powder recovered from inorganic building materials resembles the RCWCM component. Another source is the surplus cement slurry utilized during tunnel construction to reinforce the formation.

Additionally, RCWCM can be obtained from laboratory test samples. In the context of this research, the DCP was derived (see Figure 2(a)) from waste materials generated within test laboratories. Several reasons underlie this selection. First, convenience plays a crucial role as raw materials can be conveniently collected from the laboratory without incurring extra shipping costs. Second, the economic aspect is significant, as the waste cement slurry collected in this experiment has already been disposed of during testing, resulting in reduced energy consumption for waste processing and lower laboratory waste management costs. Lastly, availability is key, as test laboratories produce substantial cement-based waste annually.

The granulometry curve for DCP and OPC is presented in Figure 2(b). X-ray diffraction (XRD) analysis was performed (see Figure 2c) to evaluate the chemical arrangement of DCP, and the chemical composition of OPC, DCP, and SF is presented in Table 1. The quartz sand (QS) was acquired from the local seller, and the quartz sand was known to be sourced from the best quality sand reserves. As presented in Figure 3(a), Aerogel was purchased from the material supplier in Peshawar, Pakistan. The granulometry and physical properties of quartz sand and aerogel are provided in Figure 3(b) and Table 2. Double-hooked end steel fibers, as presented in Figure 4, were acquired from a local seller in Peshawar, Pakistan, and their physical properties are displayed in Table 3. Due to the addition of DHE-SFs, DCP, and AG,

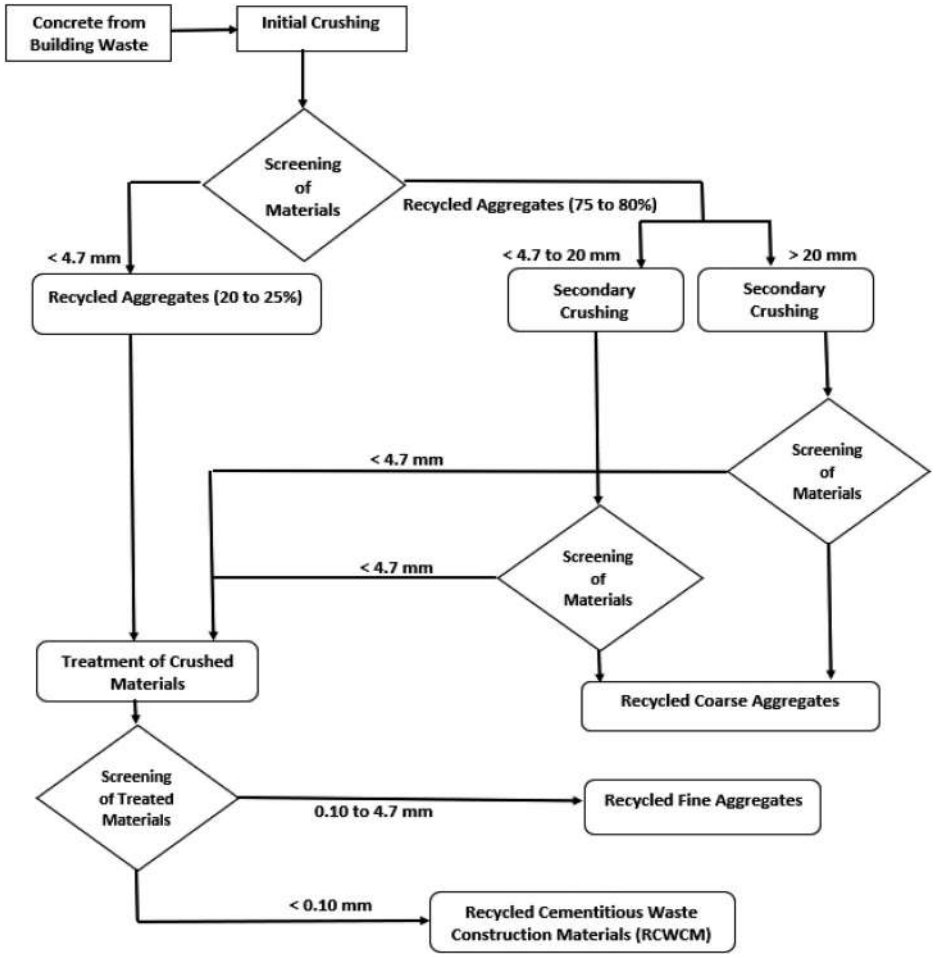

Figure 1. Flowchart diagram for the development of RCWCM.

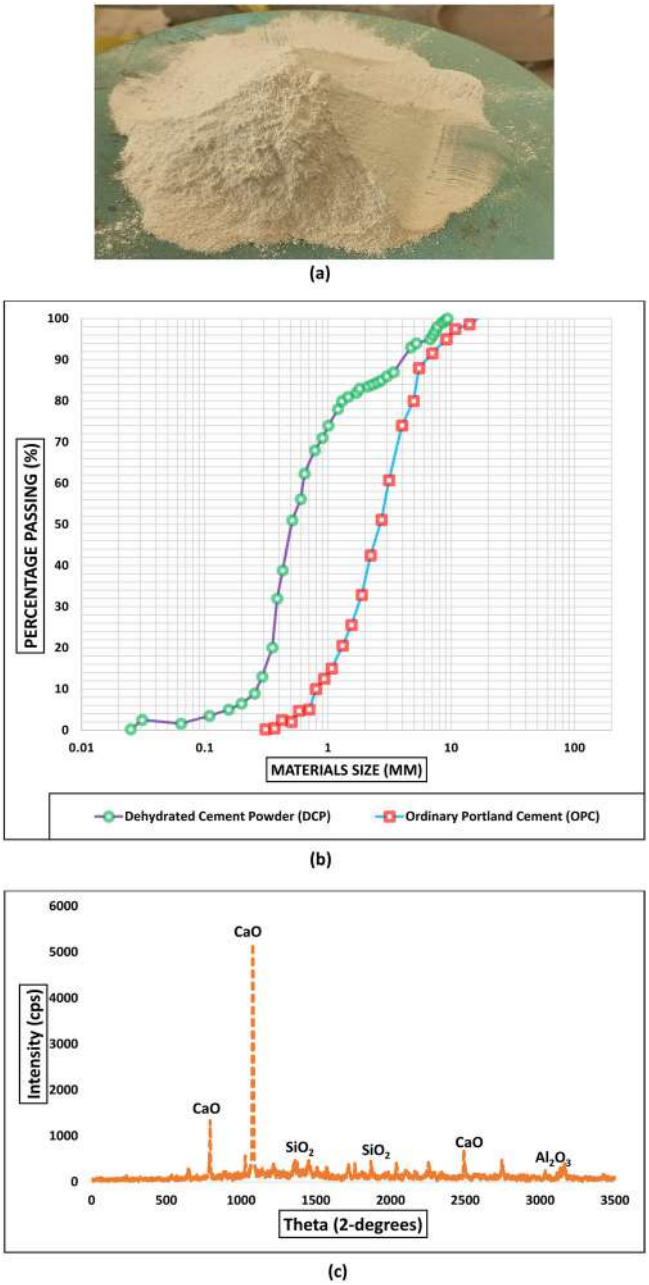

Figure 2. (a). The visual appearance of dehydrated cement powder, (b). Granulometry Curve for DCP and OPC, and (c). X-ray diffraction analysis of DCP.

Table 1. Chemical composition of OPC, DCP, and silica fume.

Component	OPC (%)	DCP (%)	Silica fume (%)
Silicon dioxide (SiO_2)	23	35.2	98.9
Calcium oxide (CaO)	63.7	46.5	0.1
Aluminum oxide (Al_2O_3)	4.1	8.9	0.1
Ferric oxide (Fe_2O_3)	3.9	2.3	0.1
Magnesium oxide (MgO)	2.6	1.8	0.1
Sulfur trioxide (SO_3)	1.9	1.1	0.1
Sodium oxide (Na_2O)	0.3	0.7	0.1
Potassium oxide (K_2O)	0.2	0.5	–
Calcium sulfate ($CaSO_4$)	0.4	0.5	–
Loss on ignition	0.1	2.5	0.5

a certain quantity of admixture was added to the mixture to maintain the water-to-cement ratio and flowability of UHPLC.

The current study developed six distinct concrete mixtures. Their comprehensive details are laid out in Table 4. Within these formulations, each mixture carried a label starting with "M," followed by a number, denoting its order. Following this, the digits after "DCP" and "AG" specify the dehydrated cement powder and aerogel used to substitute for OPC and QS in each specific mixture partially. To illustrate, a mixture that incorporates 0% DCP and 0% AG is designated as M1-DCP0-AG0. Similarly, a mix containing 5% DCP and 5% AG is identified as M2-DCP5-AG5, and this labeling pattern continues for the

(a)

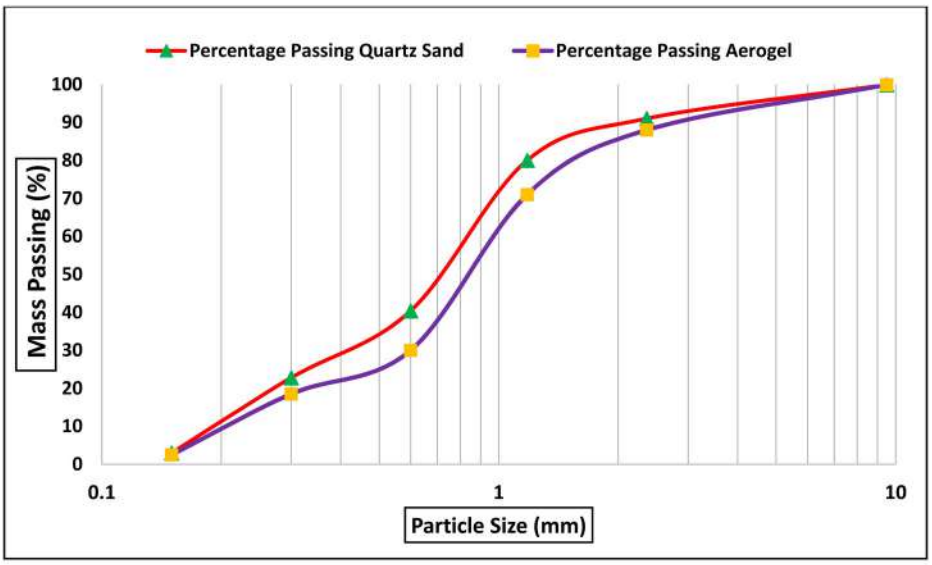

(b)

Figure 3. (a). The visual appearance of aerogel and (b) granulometry of fine aggregate and aerogel.

Table 2. Physical properties of fine aggregate and aerogel.

Property	Quartz sand	Aerogel
Density	2.66 g/cm^3	1.3 g/cm^3
Surface area	23 m^2/g	885 m^2/g
Moisture absorption	Limited moisture absorption	Highly hydrophobic
Specific gravity	2.71 g/cm^3	0.11 g/cm^3
Water absorption	Low	Minimal

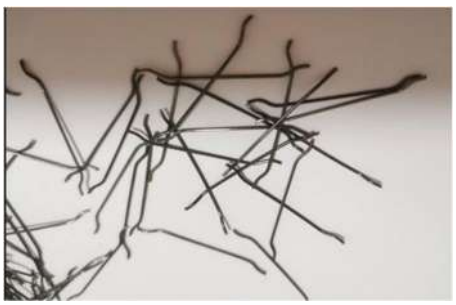

Figure 4. Double-hooked end steel fibers (DHE-SFs).

subsequent mixtures. To improve the reliability of the findings and maintain experimental consistency, the current study examined four individual samples from each specific UHPLC mixture. After testing, average values were calculated from these samples. This approach of using multiple samples was instrumental in mitigating the influence of potential anomalies, thereby refining our measurements' accuracy. The standard deviation was also computed to discern the degree of variability among the samples. This statistical measure yielded valuable insights, shedding light on the consistency and uniformity of the formulated UHPC mixtures.

Table 3. Physical properties of DHE-SFs for UHPLC.

Property	Description
Fiber shape	Double hooked end
Fiber length	30 mm
Diameter	0.6 mm
Aspect ratio	50
Tensile strength	$\geq$ 1000 MPa
Modulus of elasticity	$\geq$ 205 GPa
Density	$\geq$ 7.95 g/cm^3
Bond strength	Excellent
Compatibility	Compatible with various cementitious matrices

Table 4. Mix details of all samples of UHPLC (kg/m^3).

Mix ID	OPC	SF	DCP	QS	AG	Water	DHE-SFs	AD
M1-DCP0-AG0 (Ref)	905	320	0	1480	0	230	24.5	0.5%
M2-DCP5-AG5	859.75	320	45.25	1406	74	230	24.5	0.55%
M3-DCP10-AG10	814.5	320	90.5	1332	148	230	24.5	0.6%
M4-DCP15-AG15	791.75	320	113.25	1258	222	230	24.5	0.7%
M5-DCP20-AG20	769.25	320	135.75	1184	296	230	24.5	0.77%
M6-DCP25-AG25	746.625	320	158.375	1110	370	230	24.5	0.8%

Abbreviations: OPC: Ordinary Portland Cement; SF: Silica Fume; DCP: Dehydrated Cement Powder; QS: Quartz Silica; AG: Aerogel; DHE-SFs: Double Hooked-End Steel Fibers; AD: Admixture.

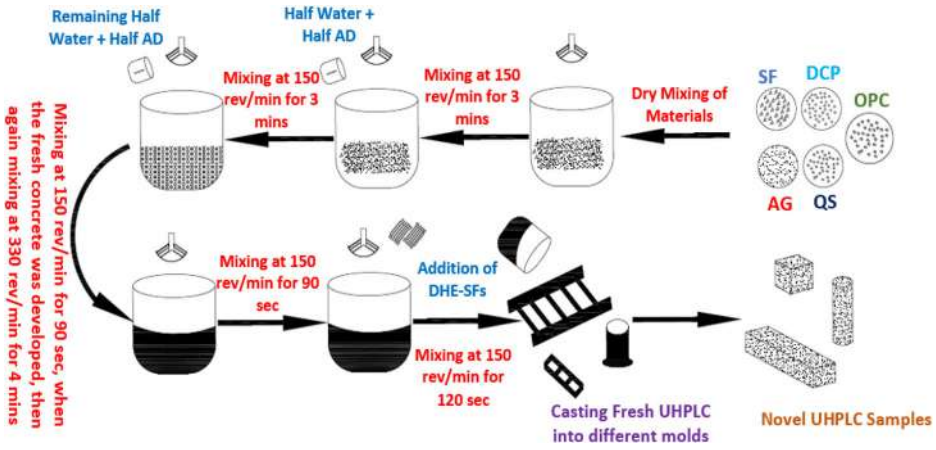

Figure 5. Method for mixing of raw materials to develop novel UHPLC.

3. Mixing of raw materials to develop UHPLC

To produce UHPLC, a systematic mixing process is crucial, accompanied by the appropriate choice of mixer. The detailed process of mixing raw materials for the development of UHPLC is presented in Figure 5. The UHPLC mixture requires a high-quality mixer for achieving thorough blending and uniform distribution of the raw materials. A high-speed, forced-action planetary mixer for UHPLC production is commonly employed. This type of mixer offers efficient mixing capabilities, ensuring proper dispersion of the materials within a relatively short duration. To commence the mixing process, the measured quantity of QS was placed in the mixing container of the high-speed planetary mixer. Subsequently, the OPC was added, and DCP can be partially substituted for OPC in varying percentages (0%, 5%, 10%, 15%, 20%, and 25%). The gradual addition of DCP to the mixture should be done while maintaining consistent mixing, ensuring proper integration of the substitute material. The mixer incorporated the AG particles as a partial replacement for QS at different percentages (0%, 5%, 10%, 15%, 20%, and 25%). Maintaining the required water-to-binder ratio with the assistance of the admixture, half of the water with half the admixtures was first added. After mixing for 3 min, the remaining water and admixture were added to develop fresh UHPLC. The mixer was then operated at the recommended speed to initiate the blending of dry components, ensuring their homogeneous distribution. Next, the DHE-SFs were introduced into the mixer while rotating. The mixing time was allowed to be sufficient to achieve the uniform dispersion of fibers throughout the mixture. All the materials were carefully added to the rotating mixer, and the mixing process continued until a homogeneous and consistent UHPLC mix was achieved.

Monitoring the mixture's consistency throughout the mixing process and adjusting the water content to attain the desired workability is crucial. Additionally, proper cleaning and preparation of the mixer between mixtures are essential to prevent cross-contamination and maintain accurate and reliable results. It's important to note that, in

the preparation of every blend, a thorough process involved extracting four exact samples, which were subsequently subjected to comprehensive testing. This protocol was methodically followed to account for variations within the blend, ensuring the results' reliability and representativeness. These samples underwent severe testing to assess a range of properties, including but not limited to strength, durability, and microstructural characteristics. The results obtained from these three samples were precisely averaged to derive a final value for each specific test. This testing and subsequent averaging method was crucial in minimizing the potential for discrepancies within individual samples, ultimately offering a more precise and dependable representation of the UHPC mixtures' performance.

4. Test methods

4.1. Microstructural analysis of UHPLC

This research conducted a comprehensive battery of tests to assess various properties of UHPLC. The mercury intrusion porosimetry method was employed to investigate pore diameter distribution and X-ray diffraction (XRD) analysis to examine the mineral composition of UHPLC, providing crucial insights into crystal structures and mineral phases present in the material. This comprehensive testing regimen thoroughly explains the UHPLC's properties and performance characteristics. XRD exposes a UHPLC sample to X-ray radiation and measures the resulting diffraction pattern. This pattern provides information about the crystal structure and mineral phases present in the UHPLC, allowing for identifying and quantifying different mineral constituents.

4.2. Flowability of UHPLC

The flowability of fresh UHPLC was examined using the slump test according to ASTM C143 [40], which involves filling a standardized cone-shaped mold with fresh concrete and measuring the slump to measure workability.

4.3. Mechanical properties of UHPLC

The compressive strength of hardened UHPLC was determined at multiple time points (28, 56, and 90 days) through ASTM C39 [41] compression tests on cylindrical specimens (300 mm × 150 mm). Bond strength, reflecting adhesion between concrete and other materials, was evaluated using the pull-out test on 150 mm x 150 mm cubical samples at 28 and 90 days (see test setup in Figure 6(a)), following ASTM C900 [42].

4.4. Functional properties of UHPLC

Thermal conductivity, a key thermal property, was determined using the guarded heat flow meter test method (ASTM C518 [43]), which measures heat transfer under steady-state conditions. Acoustic properties were evaluated using the standard test method for laboratory measurement of airborne sound transmission loss, assessing the sound transmission loss of UHPLC panels or elements subjected to sound waves at different frequencies.

4.5. Durability properties of UHPLC

Sulfate attack resistance was assessed using ASTM C1012 [33], where UHPLC specimens were subjected to a 10% sodium sulfate solution, tracking mass changes to determine sulfate resistance. Shrinkage was measured following the ASTM C157 [44] method; see the test setup for shrinkage presented in Figure 6(b), monitoring length changes of prismatic specimens. Thermal behavior was studied through thermogravimetric analysis (TGA), offering insights into heat flow, phase transitions, and weight loss under varying temperature conditions.

5. Results and discussion

5.1. Microstructural analysis of UHPLC

5.1.1. Pore structure of UHPLC

Figure 7 provides insight into the influence of varying proportions of DCP and AG on the pore structure of UHPLC at the 90-day mark. This graph plots pore diameter against dV/dlog(d), providing a nuanced understanding of how pore volume changes relative to pore diameter. Three specific mixtures were examined: the reference sample M1-DCP0-AG0, M3-DCP10-AG10, and M5-DCP20-AG20. At the onset, the mixtures showed distinct starting points around a pore diameter of 4 nanometers. The reference mixture starts at a lower dV/dlog(d) value of 0.01, whereas M3-DCP10-AG10 starts at 0.045, and M5-DCP20-AG20 begins at 0.04. These differences in the initial points suggest a varying volume of the smallest pores among the mixtures, likely due to the influence of DCP and AG. As the pore diameter increases, the curves demonstrate intriguing patterns and fluctuations. For instance, the curve representing the reference mixture approaches a value close to zero around a 10-nm pore diameter, implying a comparatively low volume of pores in this size range. Contrarily, the modified mixtures M3 and M5 maintain significant values, indicating a more substantial volume of pores within the same diameter range.

Upon thoroughly examining Figure 7, it becomes evident that the influence of varying proportions of DCP and AG on the pore structure of UHPLC at the 90-day mark is substantial and multifaceted. The initial disparities in pore volume at smaller diameters underscore the role of these additives in fine-tuning the material's microstructure. As pore size increases, the curves unveil intriguing nuances. The reference mixture exhibits a stark decline in pore volume around the 10-nanometer range, implying a scarcity of pores within this size bracket, possibly contributing to its lower permeability. In contrast, the modified mixtures, notably M3-DCP10-AG10 and M5-DCP20-AG20, maintain significantly higher pore volumes in this range, which could be indicative of enhanced permeability but also increased vulnerability to certain aggressive agents due to the prevalence of larger pores. The shifting peak positions

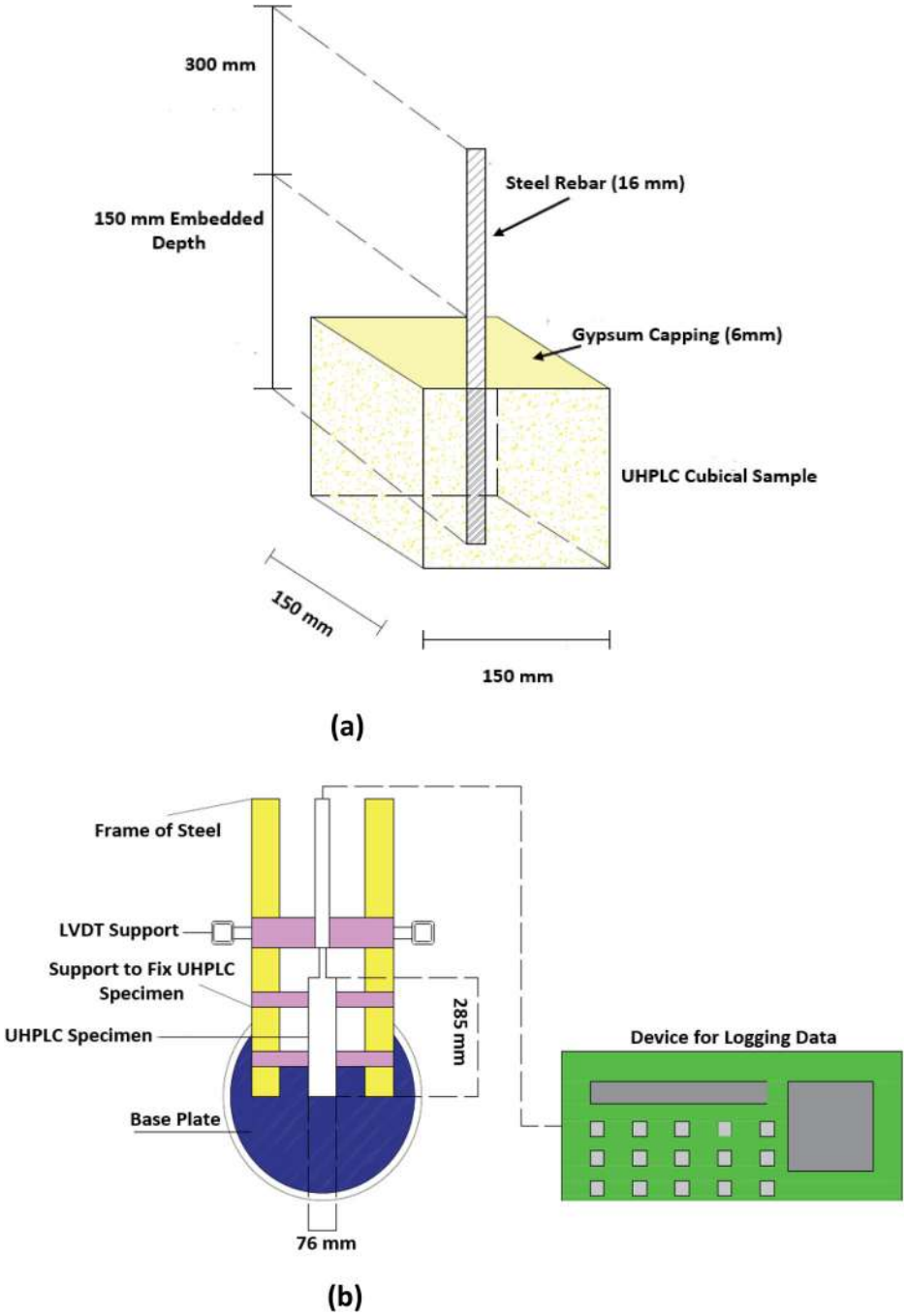

Figure 6. (a) Test setup for bonding strength of UHPLC and (b) test setup for shrinkage of UHPLC.

underscore unique pore size distributions in these mixtures, offering a route to tailoring the material's characteristics.

The peaks of the curves further clarify the different pore size distributions among the mixtures. The highest peak for the reference mixture occurs at (6, 0.05), suggesting a high volume of 6-nanometer pores. However, for M3-DCP10-AG10, the pinnacle happens at (30, 0.025), and for M5-DCP20-AG20, it occurs at (15, 0.045), each indicating a unique distribution of pore sizes distinct from the reference mixture. Beyond these peaks, the curves exhibit complex fluctuations, at times intersecting and diverging, which indicates a dynamic and diverse pore structure among these mixtures. As the pore diameter nears the upper limit of 100,000 nanometers, all the curves eventually converge to a dV/dlog(d) value of 0.05, signifying a consistent volume of larger pores across all three mixtures. The fluctuations, peak positions, and other variations can be attributed to the impact of incorporating DCP and AG as partial substitutes in the UHPLC mixtures. These modifiers appear to induce significant changes in both the distribution and volume of pores, thereby creating distinct pore structures that diverge from the reference mixture [45]. Moreover, the complex fluctuations observed across the pore diameter spectrum highlight the intricate interplay between DCP and AG and their influence on pore structure. These findings deepen our understanding of UHPLC and raise questions about how these pore structural variations may impact other properties, such as thermal conductivity or acoustic

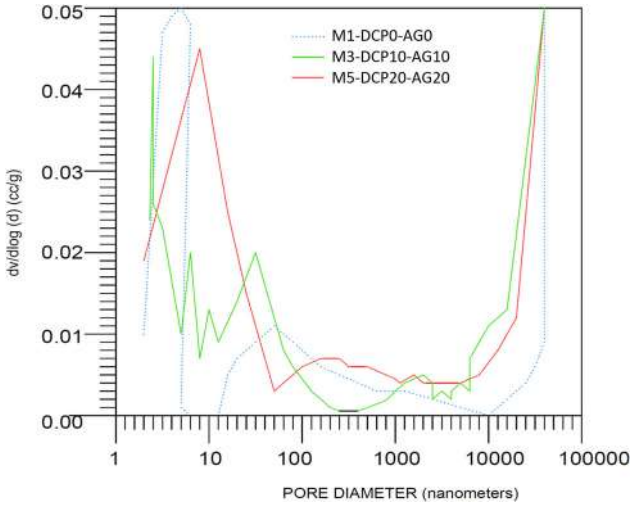

Figure 7. Pore structure of UHPC after hydrating at 90 days.

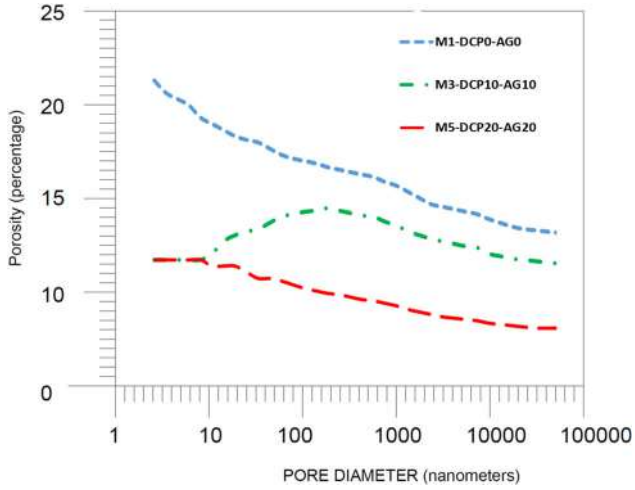

Figure 8. Porosity analysis of UHPLC at 90 days.

performance, which warrant further investigation. In essence, this analysis suggests that the introduction of DCP and AG presents a versatile approach to customizing UHPLC for specific engineering applications, with the potential to optimize both its mechanical and environmental performance.

5.1.2. *Porosity analysis of UHPLC:*

Porosity is a critical property in concrete, directly influencing its mechanical and durability characteristics. In this study, the initial porosity values of the three concrete mix designs differ significantly. As presented in Figure 8, the first line represents the sample with no DCP or aerogel substitution, starting with the highest porosity at 24.4%. This high porosity can be attributed to the absence of DCP and aerogel, which typically serve as fillers, reducing pore spaces in the concrete matrix. Figure 8 revealed distinct porosity levels among the three concrete mix designs at the outset. The first line, representing the control sample without substitutions (M1-DCP0-AG0), exhibits the highest initial porosity at 24.4%. This high porosity can be attributed to the absence of DCP and aerogel, which normally act as fillers, occupying pore spaces within the concrete matrix. In contrast, the second line (M3-DCP10-AG10) and the third line (M5-DCP20-AG20) exhibit lower initial porosity values, indicating that including DCP and aerogel has an initial positive effect on reducing porosity.

As the lines progressed along the *x*-axis, representing pore diameter in nanometers, all three samples showed a gradual reduction in porosity. This decline is mainly due to the natural compaction of the concrete matrix as it cures over time. Cement hydration, the chemical process where water reacts with cement particles to form calcium silicate hydrates (C-S-H), is crucial in filling some pores and decreasing porosity. However, the rate of this reduction remains relatively slow until we reach a critical pore diameter of approximately 85 nanometers. At the critical point (around 85 nm), there is a significant and noticeable drop in porosity for the first line (M1-DCP0-AG0). This abrupt reduction suggests that the pores within this size range are more amenable to pore-filling reactions. The C-S-H gel formation becomes particularly effective in filling these pores, resulting in a substantial decrease in overall porosity.

In contrast, the second line (M3-DCP10-AG10) and the third line (M5-DCP20-AG20) experience a less dramatic decrease in porosity at this critical pore size threshold. The presence of DCP and aerogel in these mix designs may introduce microstructural changes that influence the pore size distribution. These substitutions may create additional pore space or alter the availability of reactants, which could explain the less pronounced drop in porosity compared to the control sample. When further progressed along the *x*-axis, a consistent, gradual decrease was observed in porosity for all three lines. This continued reduction can be attributed to the ongoing curing and hydration of the concrete and the continued refinement of pore structures within the matrix. The presence of DCP and aerogel may continue to influence the pore structure, explaining the slower rate of porosity reduction observed in the second and third lines. Towards the end of the *x*-axis, all three lines exhibit a small dip or dive in their porosity values. Several factors could contribute to this phenomenon, including the inherent variability in concrete pore structures and the influence of external environmental conditions during testing. Notably, the third line (M5-DCP20-AG20), which incorporates the highest substitutions of DCP and aerogel, displays the lowest porosity values at this stage. This suggests that these materials may have a cumulative effect in reducing overall porosity as the pore structure evolves.

Porosity results illustrate the complex interplay of factors affecting porosity in UHPLC. These factors include the initial mix design, the presence of DCP and aerogel, the effectiveness of cement hydration, and the dynamic evolution of pore structures during curing. The sudden drop in porosity at around 85 nanometers highlights a critical pore size threshold for efficient pore-filling reactions. In contrast, the variations in porosity at the end of the x-axis demonstrate the intricate and multifaceted nature of concrete microstructure [46]. Further research and in-depth analysis are necessary to fully comprehend and optimize the impact of DCP and aerogel substitutions on concrete porosity across various mix designs and curing conditions.

5.1.3 *X-ray diffraction Analysis of UHPLC:*

Figure 9(a–c) illustrates the significant effects of DCP and AG as partial substitutes on the crystalline phases in UHPLC samples, as discerned through X-ray diffraction analysis. In the reference mixture M1-DCP0-AG0, Figure 9(a) reveals higher initial peaks attributed to unreacted cement phases like C-S-H (calcium-silicate-hydrate), C_2S (dicalcium silicate), C_3S (tricalcium silicate), and Portlandite ($Ca(OH)_2$). These elevated peaks point toward incomplete cementitious reactions and unhydrated cement phases.

In contrast, the modified mixtures, particularly M3-DCP10-AG10 (Figure 9(b)) and M5-DCP20-AG20 (Figure 9(c)), exhibit considerably higher peaks for the crystalline phases. This suggests enhanced hydration and more complete pozzolanic reactions attributed to adding DCP and AG. Notably, the greater presence of Portlandite, C-S-H, C_2S, and C_3S indicates more thorough hydration and an elevated cementitious reaction. The higher peaks in M3-DCP10-AG10 compared to the reference mixture are ascribable to the synergistic effects of DCP and AG. When these components are added, they encourage further hydration and facilitate the formation of additional crystalline phases. DCP expands the available cementitious material, while AG introduces a highly porous structure that aids hydration. M5-DCP20-AG20 takes it further, showing the highest peaks among all tested mixtures. Its unique blend of higher proportions of DCP and AG results in an even more extensive cementitious reaction [47]. This is likely due to a combination of greater available material and a more significant surface area for the hydration process, culminating in additional crystalline phases [48].

So, the modified mixtures demonstrate enhanced reactivity and hydration processes, thanks to the DCP and AG additives. The elevated peaks observed in these modified samples imply the fuller utilization of the cementitious material, thereby hinting at a more densely packed microstructure and potentially improved mechanical properties.

5.2. *Flowability*

Figure 10 illustrates the impact of different concentrations of DCP and AG on the flowability of UHPLC mixtures. An apparent decline in flowability was observed as the amounts of DCP and AG were incrementally introduced into the mixtures. The principal cause of this trend is the inherent characteristic of DCP to absorb water, consequently diminishing the mixture's workability. A direct correlation was established: the higher the concentration of DCP and AG incorporated, the more pronounced the reduction in flowability. The incorporation of 5% DCP and AG culminated in a flowability measurement of 276 mm, reflecting a 4.8% decrease compared to the reference mixture. In a similar trend, the flowability experienced a more substantial reduction to 251 mm, marking a 13.4% decrease when the mixture was formulated with 10% DCP and AG. This observable phenomenon can be attributed to numerous underlying factors. Initially, internal instability and rehydration processes within the DCP play a crucial role. The heating treatment instigates a transformation in the Calcium-Silicate-Hydrate structure housed within the DCP, inducing internal instability. Concurrently, elements such as calcium oxide within the DCP undergo a rehydration process, elevating water consumption levels. In the context of UHPLC mixtures, where water content is maintained constant, an augmentation in DCP content results in a swift depletion of available free water. This rapid utilization of water adversely affects the slurry's flowability and plasticity. Another key aspect influencing the reduction in flowability is the formation process of DCP. The synthesis of DCP necessitates a high-temperature treatment, which prompts the calcium-silicate-hydrate phase to depolymerize, transitioning into an oligomeric state. As a result, DCP particles exhibit a larger specific surface area than conventional

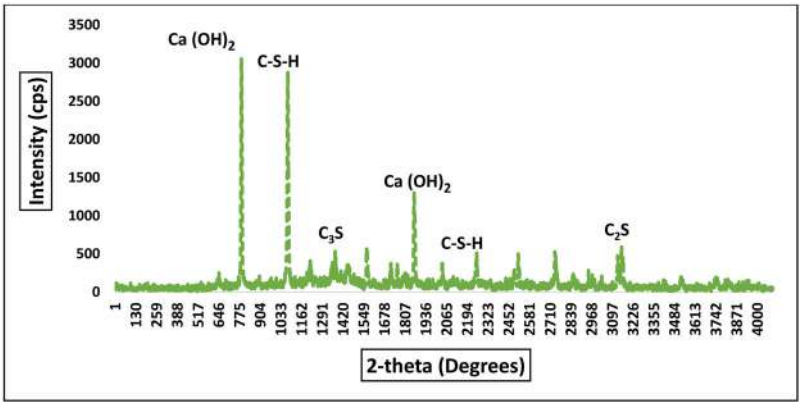

(a)

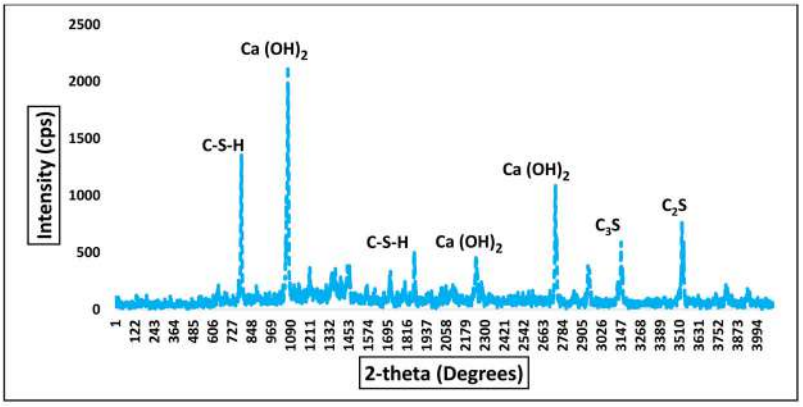

(b)

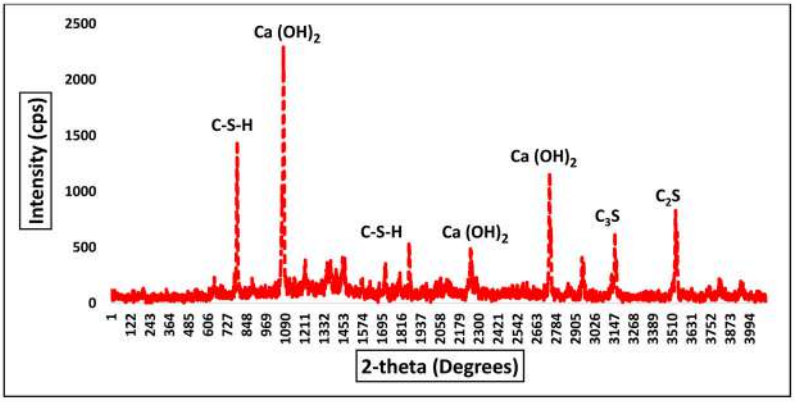

(c)

Figure 9. XRD analysis; (a) reference (M1-DCP0-AG0), (b) M3-DCP10-AG-10, and (c) M5-DCP20-AG20.

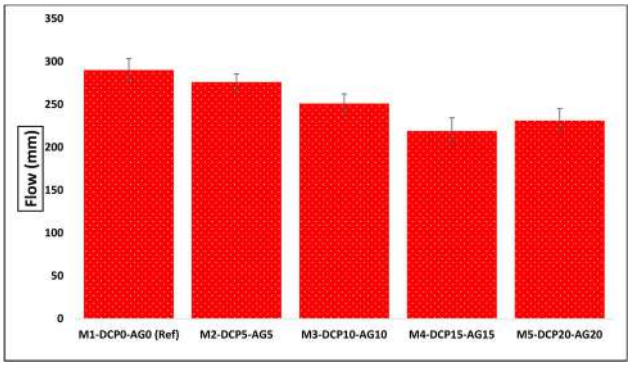

Figure 10. Flowability of UHPLC.

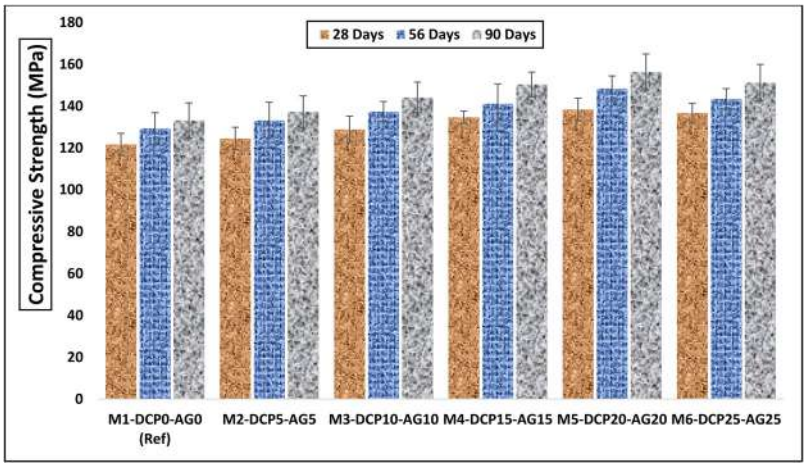

Figure 11. Compressive strength of UHPLC.

cement particles. This increased surface area promotes the formation of reconnected calcium-silicate-hydrate gel during the initial hydration phases. Due to its elevated availability, this reconnected gel exhibits a propensity to readily amalgamate with non-evaporable water, further influencing the overall characteristics of the mixture [49].

The observed trend exhibited a notable shift upon reaching a 15% dehydrated cement powder and aerogel composition. Contrary to the initial pattern of decreasing flowability, an increase was recorded. This unanticipated reversal is primarily attributed to the advantageous properties of the aerogel component incorporated into the mixture [50]. Aerogel, characterized by its lightweight and porous nature, enhances flowability by functioning as a lubricant and fostering more efficient particle movement within the mixture. Upon achieving a 15% DCP and AG blend, the mixture's flowability improved, reaching 219 mm. This marked a significant increase of 12.5% compared to the mixture containing 10% DCP and AG. However, as the concentration of DCP and AG was further increased beyond the 15% mark, the flowability began to exhibit fluctuations. At a composition of 20% DCP and AG, a slight increase in flowability was observed, with the value reaching 231 mm, reflecting a 5.5% rise compared to the 15% mixture. Also, a further increase in the proportion of DCP and AG to 25% resulted in a marginal decline in flowability, which was measured at 245 mm. This demonstrated a 6.1% decrease in comparison to the 20% mixture. Such observations underscore the impact of varying concentrations of DCP and AG on the flowability of UHPLC mixtures and how the relationship isn't linear but rather complex and multifaceted.

These essential findings illuminate the critical ways different proportions of dehydrated cement powder and aerogel influence the flowability characteristics of UHPLC mixtures. A comprehensive understanding of these influential factors is instrumental in optimizing the compositional structure of UHPLC mixtures. This optimization is crucial for enhancing the performance of the concrete while ensuring efficient workflow in practical applications, potentially leading to innovations in construction methodologies and materials.

5.3. Mechanical properties of UHPLC

5.3.1. Compressive strength of UHPLC:

Figure 11 presents the consequential impact of altering Dehydrated Cement Powder and Aerogel percentages on the compressive strength of UHPLC mixtures, assessed over distinct curing periods of 28, 56, and 90 days. The reference mixture, formulated without incorporating DCP and AG, exhibited compressive strengths of 121.7, 129.4, and 133.2 MPa for each curing interval. This progressive enhancement in strength can be attributed to the continuous hydration process that facilitates the development of a denser and more cohesive matrix within the UHPLC. However, the introduction of DCP and AG into the UHPLC mixtures manifested a distinct behavioral tendency. Including 5%, 10%, and 15% concentrations of DCP and AG resulted in a consistent escalation in compressive strength. This upward trajectory is ascribed to the advantageous impact of these additives on the densification and fortification of the UHPLC matrix. These components improve the packing density and interfacial bonding within the mixture, culminating in an augmented overall strength.

Also, at a 20% concentration of DCP and AG, the mixtures achieved peak compressive strengths of 138.4, 148.4, and 156.4 MPa at the 28, 56, and 90-day intervals, respectively. These values signify substantial increases of approximately 7.5%, 14.7%, and 17.3% compared to the reference mixture. However, a plateau effect becomes discernible beyond the 20% inclusion threshold, wherein the compressive strength commences a decline, measuring 136.8, 143.5, and 151.3 MPa at the corresponding curing durations. The decrease in compressive strength beyond the 20% threshold can be attributed to the intrinsic rehydration mechanisms of DCP, which facilitate the polymerization of oligomers and their subsequent incorporation into a networked structure. This tapering of compressive strength can also be interpreted as a result of excessive DCP and AG content, which disrupts the optimal compositional equilibrium within the UHPLC. This imbalance leads to a reduction in interparticle contact and compromises the overall structural integrity of the mixture. Consequently, there is a marginal yet significant decline

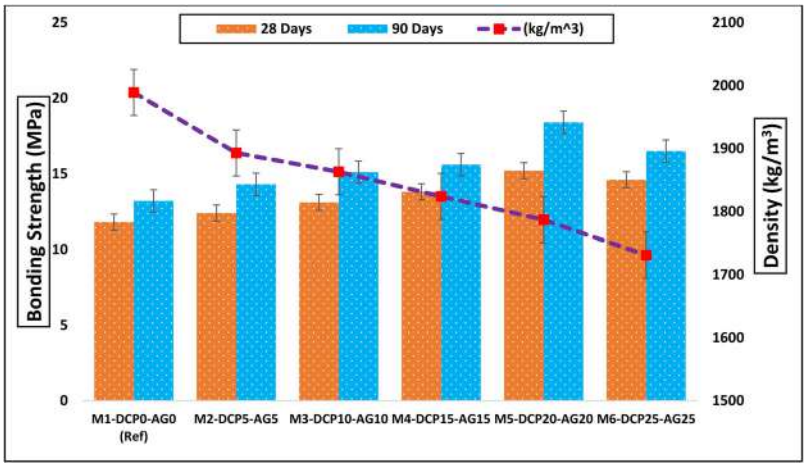

Figure 12. Bonding strength and density of UHPLC.

of approximately 0.9%, 4.4%, and 2.8% in compressive strength compared to the measurements recorded at 20% DCP and AG for the respective curing periods. This nuanced understanding of the balance between additives and compressive strength is pivotal for optimizing UHPLC mixtures in various applications [51].

The insights observed from this study can be ascribed to two inherent characteristics of DCP that markedly affect UHPLC. Initially, the tiny particles of DCP manifest a nucleation effect, amplifying the hydration process. This augmented hydration yields an increased formation of hydration products, engendering a denser microstructure within the UHPLC matrix [52]. The resultant elevated density significantly bolsters the overall compressive strength of the material. Secondly, the inherent property of DCP, characterized by its high specific surface area, enables it to absorb a substantial quantity of water. While this characteristic is advantageous in propelling the hydration process and promoting the development of hydration products, it has a downside. The proficient water absorption capacity of DCP can harm the flowability of the UHPLC mixture, potentially leading to diminished workability and an elevated risk of structural defects. As noted from the experimental results and findings disclosed in this study, a conclusion can be theorized that the integration of up to 20% DCP, along with AG, imparts a pronounced positive impact on increasing the compressive strength of UHPLC. The nucleation effect exhibited by DCP, coupled with its capacity to enhance hydration, contributes to high densification and excellent compressive strength. Nonetheless, a discernible decline in the compressive strength of UHPLC is observed when the concentration of DCP and AG surpasses the 20% mark. This decrement can be attributed to a confluence of factors, including excessive water absorption, compromised flowability, and the potential inception of defects within the structure.

Consequently, an optimal balance in the proportion of DCP and AG is imperative for achieving optimal performance, and caution must be exercised to circumvent exceeding the threshold where deleterious effects on compressive strength become apparent. A careful comprehension of the interplay between DCP content, hydration, flowability, and compressive strength is instrumental in devising UHPLC mixtures endowed with enhanced mechanical properties. By carefully harnessing the potential of DCP and acknowledging its limitations, engineers and researchers are poised to formulate UHPLC mixtures that meet the requisite performance and durability standards for a spectrum of applications, thereby expanding the horizons of construction and structural engineering.

5.3.2. *Bonding strength and density of UHPLC:*

The test results presented in Figure 12 provide valuable insights into the impact of different ratios of dehydrated cement powder and aerogel on the bonding strength of UHPLC. It was observed that the reference sample exhibited bonding strengths of 11.8 and 13.2 MPa at 28 and 90 days, respectively. Interestingly, mix M2-DCP5-AG5, which consisted of 5% DCP and 5% AG, displayed improved bonding strengths of 12.4 and 14.3 MPa at 28 and 90 days, respectively, compared to M1-DCP0-AG0. This represents a significant increase of approximately 5.1% and 8.3% in bonding strength at 28 and 90 days, respectively. The trend of improving bonding strength continued as the content of DCP and AG increased. In mix M5-DCP20-AG20, with 20% DCP and 20% AG, the measured values reached 15.2 and 18.4 MPa at 28 and 90 days, respectively. This represents a substantial enhancement of around 28.8% and 39.4% in bonding strength at 28 and 90 days, respectively, compared to the reference mixture. The improvement in bonding strength can be attributed to the unique properties and high surface area of DCP particles. These properties promote the formation of a denser and more interconnected network of hydration products within the UHPLC matrix. The enhanced interlock between the cementitious matrix and the embedded fibers improves adhesion and mechanical bonding [53].

In addition to the previously discussed mechanisms, aerogel particles further enhance the interlocking effect in UHPLC by filling voids and improving the overall packing density of the mixture. This synergistic effect between

dehydrated cement powder, aerogel, and DHE-SFs results in a more cohesive and interlocked structure, ultimately enhancing bonding strength. Studies by Ali et al. [54] have shown that including fibers in concrete samples effectively controls crack spreading, thereby enhancing the pullout strength of the fibers. Furthermore, additional investigation [40] has revealed that adding fibers improves confinement at the interface between the fibers and the concrete. This enhanced confinement further increases the bonding strength and friction within the concrete matrix. However, it is important to note that the test results indicated a reduction in bonding strength for the mixture with 25% DCP and 25% AG. The measured bonding strengths for this mixture were 14.6 and 16.5 MPa at 28 and 90 days, respectively [55,56].

Besides the mechanisms previously outlined, incorporating aerogel particles amplifies the interlocking effect within UHPLC. This is achieved by the aerogel filling void spaces and elevating the overall packing density of the mixture, thereby fostering a synergistic interaction amongst dehydrated cement powder, aerogel, and DHE-SFs. This interaction culminates in a structure characterized by increased cohesion and interlocking, which is consequential in boosting bonding strength. Research conducted by Ali et al. [54] provides empirical evidence that integrating fibers within concrete samples is efficacious in moderating the propagation of cracks. This moderation, in turn, reinforces the pullout strength of the fibers embedded within the concrete matrix. Subsequent investigation [40] has further unveiled that incorporating fibers augments confinement at the interface between the fibers and the concrete. This heightened confinement contributes to an escalation in the bonding strength and friction observed within the concrete matrix. Nevertheless, it warrants mention that the empirical findings did signify a reduction in bonding strength for the mixture constituted by 25% DCP and 25% AG. The bonding strengths quantified for this particular mixture were recorded as 14.6 and 16.5 MPa at the respective curing periods of 28 and 90 days [55,56]. These observations underscore the interaction of constituents within UHPLC mixtures and the importance of methodically optimizing the proportions of DCP and AG to optimize the structural properties of the resulting material.

A series of factors could potentially support the observed decrement in bonding strength concomitant with elevated levels of DCP and AG. Incorporating excessive quantities of DCP and AG might precipitate an imbalance within the UHPLC mixture, thereby impinging upon the overall cohesion and integrity of interfacial bonding. Furthermore, the inherently high specific surface area of both DCP and AG and their propensity for water absorption could cause a less favorable environment for forming firm bonds, culminating in diminished bonding strength. Additionally, an elevated concentration of DCP and AG may result in a microstructure characterized by diminished compactness, undermining the overall bond strength between the concrete matrix and any reinforcement. These considerations underscore the paramount importance of methodically selecting and optimizing the content of DCP and AG. Such far-sightedness is instrumental in ensuring optimal bonding strength within UHPLC mixtures. Gaining insights into this intricate interlocking mechanism and discerning the avenues through which it can be bolstered by the careful addition of DCP and AG empowers engineers and researchers to finetune the bonding strength inherent in UHPLC mixtures.

Figure 12, as presented, elucidates the variations in density observed in UHPLC mixtures with the incorporation of DCP and AG. This observed diminution in density is ascribable to many scientific factors and mechanisms at play. Introducing DCP and AG as substitutive components for cement and fine aggregate brings lightweight elements into the mixture, resulting in a surge in porosity and a corresponding decrease in density. DCP, in its powdered state, presents a larger surface area than conventional cement particles, further emphasizing the density reduction. Aerogel, inherently lightweight, also significantly diminishes the mixture's aggregate density. Furthermore, the ratios in which DCP and AG are introduced influence the packing density of the UHPLC mixture; an increase in their proportions inversely affects the available space for denser constituents like cement and fine aggregate [57]. This resultant contraction in the volume of denser components is instrumental in the overarching decrease in density. Additionally, including DCP and AG particles can instigate the formation of voids and air pockets within the mixture, further attenuating its density. The experimental data unveils a consistent decline in density concurrent with the incremental addition of DCP and AG. For example, mixtures M2-DCP5-AG5 and M4-DCP15-AG15 manifest decreases in density by approximately 4.8% and 8.3%, respectively, when compared against the reference sample. As the proportions increase to M6-DCP25-AG25, the decrement in density is markedly observed, recording an approximate reduction of 13.1% relative to the reference mixture. The role of AG particles, characterized by a lower bulk density compared to conventional fine aggregates, is pivotal in orchestrating this overall decline in density [58]. To summarize, the observed decrease in the density of UHPLC with an increase in the proportion of DCP and AG can be attributed to the introduction of lightweight components, the impact on packing density, and the creation of voids and air pockets within the mixture. These factors collectively contribute to the observed decrease in density values.

By carefully determining the appropriate proportions of these components, significant enhancements can be made to the overall performance and durability of UHPLC. This refined understanding and strategic application make UHPLC suitable for diverse applications, particularly those necessitating excellent bonding capabilities and uncompromised structural integrity. In this way, the knowledge collected from studying the interactions and impacts of DCP and AG in UHPLC mixtures is crucial for advancing the field and increasing the applicability of this useful composite material.

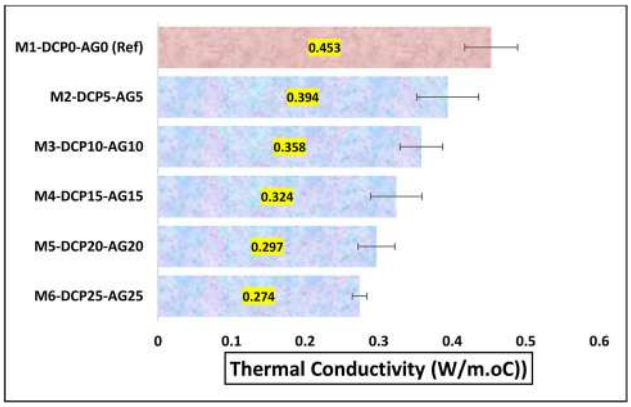

Figure 13. Thermal conductivity of UHPLC.

5.4. *Functional properties of UHPLC*

5.4.1. *Thermal conductivity of UHPLC:*

As detailed in Figure 13, the thermal conductivity tests performed on UHPLC samples with different DCP and AG concentrations produced notable variations in thermal conductivity values. The reference mixture, M1-DCP0-AG0, consistently ranked highest in thermal conductivity, with a 0.453 W/m·°C value. This high value underscores the reference mixture's relative inefficiency in thermal insulation, setting the baseline for comparisons with modified mixtures. On the other end of the spectrum, the M6-DCP25-AG25 mixture presented the lowest thermal conductivity value, clocking in at 0.274 W/m·°C. This marked reduction in thermal conductivity, nearly 39.5% lower than the reference mixture, emphasizes the effective synergistic action of DCP and AG in enhancing the material's thermal properties. The other modified mixtures—M2-DCP5-AG5, M3-DCP10-AG10, M4-DCP15-AG15, and M5-DCP20-AG20—displayed incremental improvements in thermal conductivity, with values of 0.394, 0.358, 0.324, and 0.297 W/m·°C, respectively. The descending order of these values indicates a trend: as the proportions of DCP and AG increase, the thermal conductivity of the UHPLC material decreases. Specifically, these intermediate mixtures serve as valuable data points, showing a continuum of improved thermal properties with increasing percentages of DCP and AG.

Analyzing the percentage decrease in thermal conductivity compared to the preceding mixture, it can be observed that each subsequent modification with increased proportions of DCP and AG contributed to a notable reduction in thermal conductivity. The percentage decrease in thermal conductivity values ranged from approximately 9.5% to 25.3% compared to the preceding mixture. This indicates a cumulative effect of incorporating DCP and AG in decreasing the thermal conductivity of UHPLC. The observed variations in thermal conductivity can be attributed to the influence of DCP and AG on the heat transfer properties of the UHPLC. The reference mixture, lacking the presence of DCP and AG, exhibited higher thermal conductivity due to the absence of insulating materials. Without these modifiers, the concrete matrix has higher thermal conductivity, allowing heat to be conducted more readily through the material [36, 39]. The M6-DCP25-AG25 mixture emerges as a standout in thermal conductivity, recording the lowest values in this performance metric. This specific formulation reduces thermal conductivity at a 25% inclusion rate for both DCP and AG. This heightened concentration of DCP and AG doesn't merely act as filler or partial replacement but takes on a more dynamic role in manipulating the UHPLC's thermal properties. For instance, DCP, when used as a partial replacement for Ordinary Portland Cement, contributes to reduced thermal conductivity by altering the concrete's core composition. Simultaneously, AG, known for its insulating attributes, reinforces the UHPLC's resistance to heat transfer [59]. This dual action of DCP and AG optimizes the material's thermal behavior: DCP ameliorates the concrete by acting as a fractional substitute for OPC, thereby diminishing the material's innate thermal susceptibility. AG complements this by providing an insulating layer that effectively hampers heat transfer through the concrete matrix. As a result, the combined effect is a synergistic improvement in thermal performance, characterized by markedly lower thermal conductivity values [59].

These findings suggest that the M6-DCP25-AG25 mixture is particularly well-suited for applications that require both strength and thermal efficiency, offering a new prospect for materials science to explore concrete formulations that are firm and thermally resilient. Therefore, incorporating DCP and AG in this specific proportion may serve as a blueprint for developing future UHPLC formulations for demanding thermal applications.

5.4.2. *Acoustics performance of UHPLC*

The acoustics test results for all UHPLC samples in the scope of determined frequency (450– 5950 Hz) are presented in Figure 14; during the sound absorption (acoustics) test conducted on the UHPLC samples, which were modified with different proportions of DCP and AG, distinct variations in sound absorption coefficient values were observed. The reference mixture (M1-DCP0-AG0) consistently exhibited lower sound absorption coefficients across the tested frequency range, whereas the sample M6-DCP25-AG25 demonstrated higher sound absorption coefficients. Similarly, the other modified mixtures, M2-DCP5-AG5, M3-DCP10-AG10, M4-DCP15-AG15, and

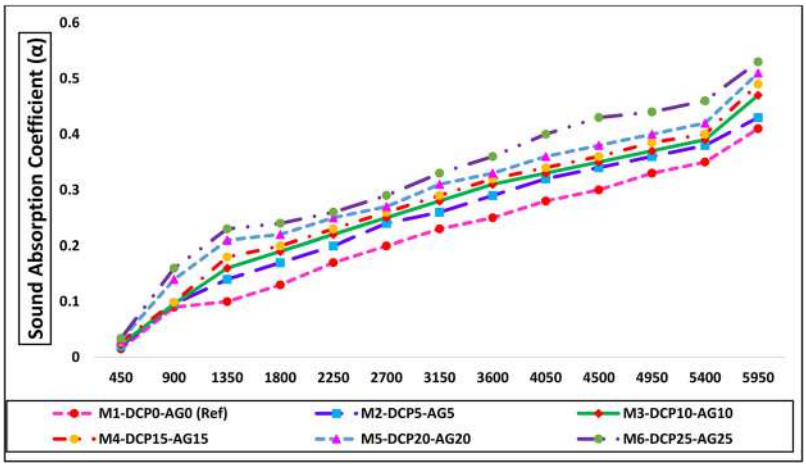

Figure 14. Sound absorption of UHPLC.

M5-DCP20-AG20, displayed further improved sound absorption performance compared to the reference mixture. When the scope was lower than 1350 Hz, the coefficient for sound absorption had almost similar values for all the mixtures. Though the mixtures with DCP and AG had an enhanced coefficient for sound absorption as compared to the reference mixture, no notable difference was observed amongst all the samples, such as at the frequency range of 900 Hz, the coefficient for sound absorption values for M1-DCP0-AG0, M2-DCP5-AG5, M3-DCP10-AG10, M4-DCP15-AG15, M5-DCP20-AG20, and M6-DCP25-AG25 were 0.090, 0.094, 0.096, 0.099, 0.14, and 0.16, respectively. When the frequency was higher than 3600 Hertz, the coefficient for sound absorption increased with the increasing frequency. This represents the strong influence of frequencies on the coefficient of sound absorption [60]. Under similar frequencies, the UHPLC mixtures with DCP and AG depicted a greater sound absorption coefficient than the reference mixture at each frequency range.

The M6-DCP25-AG25 mixture, incorporating the highest concentration of DCP and AG, emerged as the most exceptional acoustic performance formulation, boasting the highest sound absorption coefficients among all tested samples. The inclusion of AG at this increased concentration played a pivotal role in enhancing the UHPLC's sound absorption capabilities. The material's characteristics contribute to a more significant attenuation and dissipation of sound energy, resulting in markedly higher sound absorption coefficients. A trend becomes evident when examining the increment in sound absorption coefficients across the various mixtures. Each progressive formulation, characterized by increased proportions of DCP and AG, registered a noticeable upswing in sound absorption capabilities. This percentage increase ranged from approximately 4.9% to 7.8% compared to its immediate predecessor in the sequence of mixtures. This data illustrates the cumulative benefit of integrating DCP and AG into the UHPLC matrix. As the proportion of these modifiers increases, so does the mixture's ability to attenuate and dissipate sound energy, enhancing its overall acoustic performance. The results underscore the potential of DCP and AG as key ingredients for engineering UHPLC formulations optimized for superior acoustic properties.

The enhancement in acoustic properties of the UHPLC mixtures can be attributed to including DCP and AG as modifier components. The reference mixture, which did not incorporate DCP and AG, exhibited limited sound absorption capabilities. This is largely because it lacked elements conducive to sound energy dissipation and reduction, as evidenced by its consistently lower sound absorption coefficients across various frequency ranges [21, 61]. In comparison, the modified UHPLC mixtures, which included varying proportions of DCP and AG, displayed significantly improved sound absorption performance. DCP and AG serve as effective, sound-absorbing materials within the UHPLC matrix. Their inclusion increases the surface area for sound wave interaction and enriches the material's sound energy dissipation and scattering capacity. Specifically, DCP's fine particulate nature and AG's unique structural characteristics create a more complex pathway for sound waves, leading to increased attenuation and absorption of sound energy.

These attributes contribute to higher sound absorption coefficients in the modified mixtures across the entire frequency spectrum. Essentially, DCP and AG enhance the acoustic properties of the UHPLC by promoting better energy absorption and dissipation mechanisms, setting a new standard for concrete mixtures where acoustic performance is a crucial consideration.

5.5. *Durability properties of UHPLC*

5.5.1. *Sulfate attack on UHPLC:*

Figure 15(a, b) presents the behavior of UHPLC under a sulfate environment in terms of mass loss and residual compressive strength. The sulfate attack test results provide valuable insights into the resistance to sulfate attack and durability of the modified UHPLC mixtures. Among these mixtures, the M5-DCP20-AG20 mixture demonstrates superior performance, exhibiting the lowest mass loss (7.09%) and the highest retention in compressive strength (145.3 MPa). This exceptional performance can

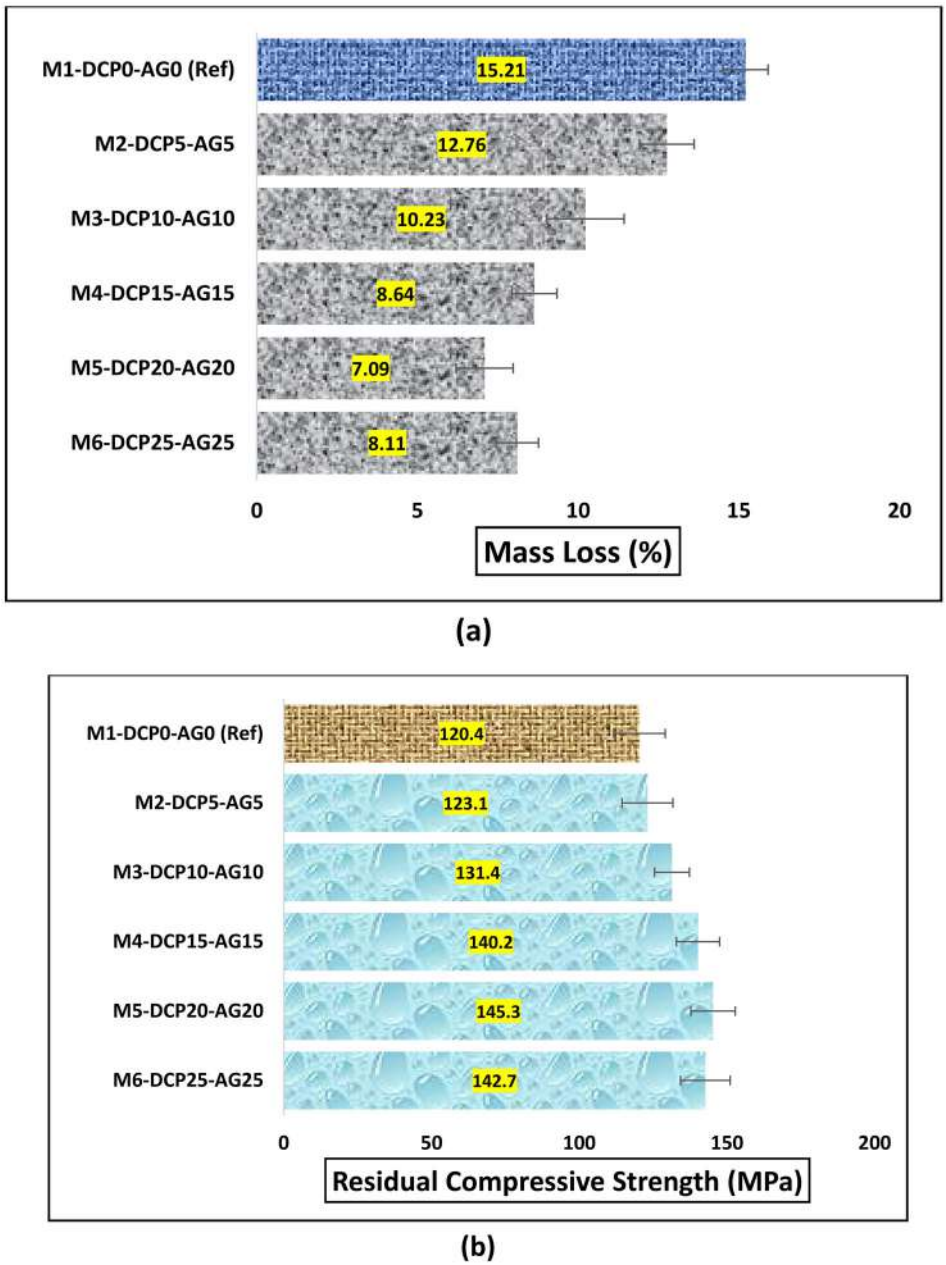

Figure 15. Effect of sulfate attack on UHPLC: (a) mass loss and (b) residual compressive strength.

be attributed to various factors and interactions within the concrete system. Incorporating DCP and AG in the UHPLC mixtures significantly improves their resistance to sulfate attack. DCP acts as a partial substitute for cement, leading to the refinement of the microstructure and the formation of hydration products [62]. As a result, a densely packed matrix with reduced porosity is formed, enhancing the overall durability [63]. AG, on the other hand, replaces fine aggregate and contributes to the lightweight nature of the concrete. By doing so, it aids in reducing the permeability of the concrete, preventing the ingress of sulfate ions, and mitigating their detrimental effects [64]. These combined effects contribute to the outstanding performance of the M5-DCP20-AG20 mixture, demonstrating its ability to withstand sulfate attack while maintaining high compressive strength.

The results obtained from the experimentation reveal interesting trends when compared to the reference mixture (M1-DCP0-AG0). The reference mixture displayed a residual compressive strength of 120.4 MPa. Upon adding 5% DCP and 5% AG (M2-DCP5-AG5), there was a slight increase in residual compressive strength, approximately 1.9% higher than the reference mixture. However, as the proportions of DCP and AG increased, the residual compressive strength experienced significant improvements. M3-DCP10-AG10 showcased a notable increase of approximately 9.1% compared to the reference mixture. Furthermore, M4-DCP15-AG15 exhibited a substantial increase, with a percentage increase of about 16.2% compared to the reference mixture. Finally, the mixture M5-DCP20-AG20 displayed the highest compressive strength retention, with an exceptional percentage increase of approximately 20.8% compared to the reference mixture. This indicates that the addition of 20% DCP and 20% AG had a pronounced positive effect on the residual compressive strength of UHPLC. This can be attributed to the

optimum balance achieved with this specific proportion, resulting in a highly compact matrix with minimal voids. Furthermore, including DHE-SFs in all mixtures significantly enhances their resistance to sulfate attack. By effectively controlling crack propagation, DHE-SFs minimize pathways for sulfate ion ingress and mitigate the risk of damage. The synergistic effect of DCP, AG, and DHE-SFs contributes to the overall durability and sulfate resistance of the modified UHPLC mixtures. Analyzing the specific percentages used, a discernible trend emerges regarding mass loss and residual compressive strength. As the proportions of DCP and AG increase from 5% to 20% in the mixtures, there is a consistent reduction in mass loss and a gradual improvement in residual compressive strength. This trend highlights the beneficial impact of higher DCP and AG contents in enhancing the sulfate resistance of UHPLC [65]. The denser microstructure and reduced permeability resulting from increased DCP and AG proportions effectively impede the penetration of sulfate ions into the concrete, thus mitigating damage and preserving its structural integrity.

5.5.2. *Shrinkage effect on UHPLC:*

Figure 16 illustrates the effect of DCP and AG on the shrinkage performance of UHPLC. It is evident that adding DCP and AG as fractional replacements for OPC and fine aggregate significantly influences the shrinkage behavior of UHPLC. During the 180-day shrinkage test, the reference mixture (M1-DCP0-AG0) exhibited the highest shrinkage values at all curing days, reaching 2175 μ at 180 days. This can be attributed to the absence of DCP and AG, which are known to reduce shrinkage in concrete. However, as the proportions of DCP and AG increased in the modified mixtures, a noticeable decrease in shrinkage values was observed. The incorporation of DCP and AG reduced the water demand and improved the overall microstructure of the concrete, thereby mitigating shrinkage. Among all the mixtures, M6-DCP25-AG25 showed the lowest shrinkage values, measuring only 958 μ at 180 days. This significant reduction in shrinkage can be attributed to the combined effects of DCP and AG. DCP reduces the water-cement ratio, creating a denser matrix with reduced capillary porosity [66]. This, in turn, minimizes moisture loss and shrinkage. On the other hand, AG's porous structure acts as an internal reservoir for water, supplying a continuous source of moisture to the concrete during drying [67]. This internal curing effect further mitigates shrinkage by limiting the formation of microcracks and restraining volume changes [68].

Analyzing the percentage decrease in shrinkage compared to the preceding mixture reveals that each subsequent modification with increased proportions of DCP and AG contributed to a significant reduction in shrinkage. The percentage decrease in shrinkage values ranged from approximately 11.7% to 31.5% compared to the preceding mixture, indicating the cumulative effect of incorporating DCP and AG in mitigating shrinkage. The lower shrinkage values observed in the modified mixtures, particularly in M6-DCP25-AG25, can be attributed to the enhanced microstructural characteristics of the concrete. These include reduced capillary porosity, improved hydration, and controlled moisture content. These factors establish a more stable and resilient concrete matrix, resulting in lower shrinkage and improved dimensional stability over time [45]. The findings highlight the significant role that DCP and AG play in optimizing the microstructure and composition of UHPLC, leading to desirable mechanical properties such as high residual compressive strength and reduced shrinkage.

5.5.3. *Thermal analysis of UHPLC*

Figure 17 presents the impact of rising temperatures on the mass loss characteristics of UHPLC mixtures, revealing a directly proportional relationship between temperature intensities and mass loss. The reference mixture (M1-DCP0-AG0) emerged as the most thermally vulnerable sample, while M5-DCP20-AG20 outperformed all other modified mixtures regarding thermal resilience. This stark contrast in thermal behavior can be largely ascribed to the incorporation of DCP and AG, both of

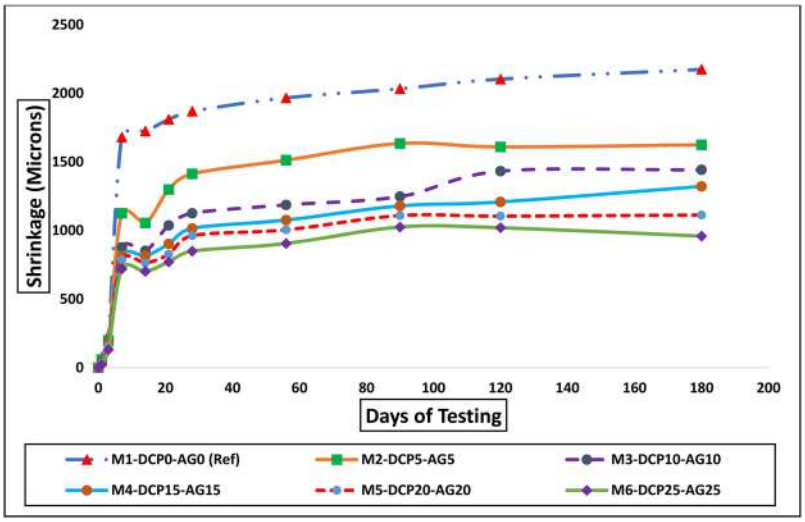

Figure 16. Shrinkage of UHPLC.

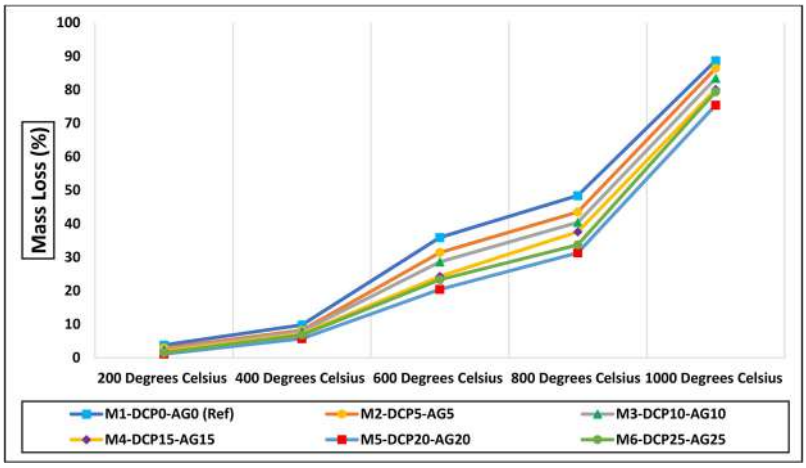

Figure 17. Mass loss in UHPLC.

which modify the inherent thermal properties of UHPLC. When introduced into the UHPLC matrix, DCP serves a dual function as it acts as a filler and a partial cement substitute, consequently lowering the concrete's overall susceptibility to heat-induced damage. AG amplifies this effect, leveraging its remarkable insulating properties and low thermal conductivity to minimize heat transfer within the concrete, enhancing its thermal stability, as cited in reference [69]. The M1-DCP0-AG0 reference mixture persistently suffered the highest mass loss across diverse temperature brackets, registering mass loss percentages of 3.8%, 9.8%, 35.9%, 48.4%, and a staggering 88.7% at 200, 400, 600, 800, and 1000 °C respectively. In stark contrast, M5-DCP20-AG20 exhibited significantly reduced mass loss, with values of 1.1%, 5.7%, 20.4%, 31.3%, and 75.4% at the corresponding temperature tiers. Other modified mixtures, including M2-DCP5-AG5, M3-DCP10-AG10, M4-DCP15-AG15, and M6-DCP25-AG25, also demonstrated marked improvements over the reference sample in thermal resistance across all tested temperatures. These findings indicate not only the efficacy but also the synergistic effect of DCP and AG in elevating the thermal resilience of UHPLC, affirming their suitability for applications requiring enhanced thermal properties. The reduced mass loss at elevated temperatures, particularly in M5-DCP20-AG20, attests to the successful mitigation of thermal vulnerabilities, thereby offering new avenues for the engineering and optimization of UHPLC for thermally challenging environments.

The reference mixture's vulnerability to thermal degradation indicates its compositional limitations, lacking the reinforcing effects of DCP and AG. Absent these influential modifiers, the concrete becomes susceptible to thermal cracking and structural weakening upon exposure to elevated temperatures, as corroborated by research findings [70]. Conversely, the modified UHPLC mixtures, fortified with varying concentrations of DCP and AG, consistently outperformed the reference mixture in thermal resilience. The lesser mass loss percentages across all temperature strata in these modified mixtures demonstrate their enhanced capacity to resist thermal degradation, a proposition supported by additional scientific literature [71]. The percentage decrease in mass loss from one modified mixture to the next reveals a compelling narrative. The data shows that each progressive increment in the proportion of DCP and AG yielded noteworthy declines in mass loss, with percentage reductions ranging from approximately 42.1% to an impressive 68.2%. This data suggests a cumulative, perhaps even synergistic, effect of DCP and AG on the thermal performance of UHPLC, strengthening its resilience against heat-induced deterioration. M5-DCP20-AG20, distinguished for its lowest mass loss values at each temperature level, merits particular attention. This mixture seems to represent an optimal balance in the ratio of DCP to AG, at 20% concentration for each. This optimized formulation yielded a more effective thermal barrier, sharply reducing heat transfer through the UHPLC matrix. As a result, the M5-DCP20-AG20 mixture was demonstrably more resistant to mass loss even under the rigors of elevated temperatures. Therefore, the results indicate that optimal proportions of DCP and AG not only reinforce the UHPLC against thermal damage but may also be fine-tuned to offer superior performance, opening new pathways for material scientists and engineers to explore tailored applications requiring robust thermal properties.

6. Sustainability aspect of current study

The development of UHPLC with modified compositions, incorporating DCP and AG as partial substitutes for cement and fine aggregate, has significant implications from a sustainability and environmental perspective. This study addresses several key challenges in the construction industry by creating a novel, low-carbon UHPLC with enhanced properties.

From a sustainability standpoint, utilizing DCP and AG as cement and fine aggregate substitutes offers multiple benefits. Cement production is a major source of carbon dioxide emissions, and by reducing the amount of cement required in the mixtures, the overall carbon footprint of concrete production can be significantly reduced. Moreover, DCP and AG are typically derived from industrial byproducts or waste materials, which reduces the demand for natural raw materials and helps minimize

waste generation [53, 72–75]. By repurposing these materials, the study contributes to the circular economy and reduces environmental impact. The low thermal conductivity of UHPLC mixtures has important implications for energy efficiency in buildings and infrastructure. Buildings are responsible for significant global energy consumption, and improving their thermal performance is crucial for reducing greenhouse gas emissions. UHPLC's low thermal conductivity improves insulation, reducing heat transfer through walls and floors. This translates to lower energy requirements for heating and cooling, reducing carbon emissions and energy costs. The socio-economic impact of this development is substantial, as it can lead to lower operating expenses for building owners and improved comfort for occupants [1, 76,77].

The enhanced sound absorption properties of UHPLC contribute to creating more sustainable and comfortable living environments. Controlling noise pollution is vital in urban areas, where high-rise buildings, long-span bridges, and tunnels are prevalent. UHPLC's ability to absorb and dampen sound waves helps mitigate noise disturbances, improving the quality of life for residents and workers. Reduced noise pollution can positively impact productivity, concentration, and overall well-being. Additionally, the construction of noise barriers using UHPLC can have socio-economic benefits by enhancing public spaces, attracting investments, and improving the livability of urban areas. In marine environments, the durability and dense microstructure of UHPLC is particularly advantageous. Structures exposed to seawater or other corrosive agents require high-performance materials to ensure longevity and minimize maintenance costs [78]. UHPLC's superior resistance to chloride ingress and chemical attack enhances the durability of marine structures, reducing the need for frequent repairs and replacements. This contributes to cost savings and ensures the safety and integrity of critical infrastructure in marine environments.

Developing low-carbon UHPLC with improved properties aligns with sustainable construction practices and addresses several environmental and socio-economic challenges [79–81]. By reducing the carbon footprint, improving energy efficiency, enhancing acoustic performance, and providing durable solutions [82], UHPLC has the potential to revolutionize the construction industry. Embracing these advancements can lead to more sustainable and resilient high-rise buildings, long-span bridges, tunnels, and marine structures, promoting socio-economic development while minimizing environmental impact [83,84].

7. Suggestions for future researches

The following suggestions are recommended for future research based on the present study.

7.1. Structural behavior and design optimization

Investigate the structural behavior of UHPLC elements, such as beams, columns, and slabs, under different loading conditions. Explore innovative design approaches and optimization techniques to fully exploit the material's high strength and lightweight properties, enabling the development of more efficient and sustainable structural systems.

7.2. Cost analysis

Conduct a thorough cost analysis to evaluate the economic viability of using UHPLC in various construction applications. Assess the costs associated with materials, production, construction, and maintenance over the life cycle of structures to determine the economic benefits and cost-effectiveness of UHPLC compared to conventional concrete.

7.3. Construction techniques and guidelines

Develop construction techniques, guidelines, and best practices specific to UHPLC to facilitate widespread adoption in real-world construction projects. This includes recommendations for mixing, placing, and curing UHPLC and quality control and assurance guidelines during construction.

7.4. Multi-disciplinary collaboration

Encourage collaboration between researchers, engineers, architects, material scientists, and industry stakeholders to foster interdisciplinary research and innovation in UHPLC. This collaboration can help bridge the gap between academia and industry, facilitating knowledge and technology transfer to practical applications.

7.5. Field studies and case studies

Conduct field studies and case studies to monitor and evaluate the performance of UHPLC in real construction projects. This will provide valuable data on the material's behavior in actual conditions and help validate laboratory findings. It will also serve as a basis for further optimization and improvement of UHPLC mixtures.

By performing research in these areas, researchers can progress the development and application of UHPLC, contributing to sustainable construction practices, improved infrastructure performance, and a reduced environmental footprint in the built environment.

8. Conclusions

This study emphasized developing novel, low-carbon, UHPLC with DCP and AG as partial substitutes. The physical, durability, functional, and microstructural properties of UHPLC are assessed. The following conclusions are presented based on the present study.

- Higher DCP and AG proportions increased flowability reduction, exemplified by a 4.8% decrease with 5% DCP and AG.
- Incorporating 5%, 10%, and 15% DCP and AG improved strength due to enhanced packing and bonding, with peak compressive strength around

7.5%, 14.7%, and 17.3% higher at 20% DCP and AG.
- Bonding strength notably increased in mix M5-DCP20-AG20, surpassing the reference mixture by 28.8% and 39.4% at 28 and 90 days, respectively.
- Higher DCP and AG proportions gradually reduced density; for instance, M2-DCP5-AG5 and M4-DCP15-AG15 decreased density by about 4.8% and 8.3% compared to the reference sample.
- In the sulfate attack, 5% DCP and AG slightly increased compressive strength by 1.9%, while M5-DCP20-AG20 exhibited a remarkable 20.8% strength increase compared to the reference mixture.
- Shrinkage decreased noticeably with increased DCP and AG proportions, from the reference mixture's 2175 μ to 958 μ in modified mixtures.
- Mass loss at elevated temperatures was highest in the reference mixture (3.8–88.7%) and lowest in M5-DCP20-AG20 (1.1–75.4%).
- Thermal conductivity ranged from 0.453 W/m·°C (reference) to 0.274 W/m·°C (M6-DCP25-AG25), with intermediate values in other mixtures.
- In pore structure analysis, mixtures exhibited distinct starting points at 4 nanometers with varying dV/dlog(d) values, impacting pore distribution and implying diverse microstructures.

Acknowledgements

The authors extend their appreciation to the Deanship of Scientific Research at King Khalid University for funding this work through a large group Research Project under grant number RGP2/351/44.

Disclosure statement

No potential conflict of interest was reported by the authors.

Funding

The authors extend their appreciation to the Deanship of Scientific Research at King Khalid University for funding this work through a large group Research Project under grant number RGP2/351/44.

Data availability statement

The data are available from the corresponding author upon request.

Ethical approval

All authors approve that the research was performed under all the ethical norms.

Consent to publish

All authors consent to publish this paper.

References

[1] Luan C, Zhang Q, Wu Z, et al. Uncovering the role of hydrophobic silica fume (HPS) in rheology, hydration, and microstructure of ultra-high-performance concrete (UHPC). J Sustain Cem Mater. 2023;12(11):1399–1413. doi: 10.1080/21650373.2023.2222398.
[2] Zaid O, Zamir Hashmi SR, El Ouni MH, et al. Experimental and analytical study of ultra-high-performance fiber-reinforced concrete modified with egg shell powder and nano-silica. J Mater Res Technol. 2023;24:7162–7188. doi: 10.1016/j.jmrt.2023.04.240.
[3] Althoey F, Zaid O, Martínez-García R, et al. Ultra-high-performance fiber-reinforced sustainable concrete modified with silica fume and wheat straw ash. J Mater Res Technol. 2023;24:6118–6139. doi: 10.1016/j.jmrt.2023.04.179.
[4] Du J, Meng W, Khayat KH, et al. New development of ultra-high-performance concrete (UHPC). Compos Part B Eng. 2021;224:109220. doi: 10.1016/j.compositesb.2021.109220.
[5] Rong Z, Wang Y, Jiao M. Optimization design and microstructure analysis of ultra-high performance cement-based composites. J Sustain Cem Mater. 2023;12(11):1376–1386. doi: 10.1080/21650373.2023.2219263.
[6] Salahaddin SD, Haido JH, Wardeh G. The behavior of UHPC containing recycled glass waste in place of cementitious materials: a comprehensive review. Case Stud Constr Mater. 2022;17:e01494. doi: 10.1016/j.cscm.2022.e01494.
[7] Schmidt MF. 2013. Sustainable building with ultra-high performance concrete (UHPC) – coordinated research program in Germany.
[8] Khan MA, Ayub Khan S, Khan B, et al. Investigating the feasibility of producing sustainable and compatible binder using marble waste, fly ash, and rice husk ash: a comprehensive research for material characteristics and production. Results Eng. 2023;20:101435. doi: 10.1016/j.rineng.2023.101435.
[9] Randl N, Steiner T, Ofner S, et al. Development of UHPC mixtures from an ecological point of view. Constr Build Mater. 2014;67:373–378. doi: 10.1016/j.conbuildmat.2013.12.102.
[10] Abdulkareem OM, Ben Fraj A, Bouasker M, et al. Mixture design and early age investigations of more sustainable UHPC. Constr Build Mater. 2018;163:235–246. doi: 10.1016/j.conbuildmat.2017.12.107.
[11] Qian D, Yu R, Shui Z, et al. 2020. A novel development of green ultra-high performance concrete (UHPC) based on appropriate application of recycled cementitious material.
[12] Abdellatief M, Elrahman MA, Elgendy G, et al. Response surface methodology-based modelling and optimization of sustainable UHPC containing ultrafine fly ash and metakaolin. Constr Build Mater. 2023;388:131696. doi: 10.1016/j.conbuildmat.2023.131696.
[13] Lu J-X, Ali HA, Jiang Y, et al. A novel high-performance lightweight concrete prepared with glass-UHPC and lightweight microspheres: towards energy conservation in buildings. Compos Part B Eng. 2022;247:110295. doi: 10.1016/j.compositesb.2022.110295.
[14] Head PR, Cerib MD, Industry FC, et al. Ultra high performance concrete with ultrafine particles other than silica fume, in: third int. Symp UHPC. 2012; 2012:213–225.
[15] Kılıç A, Atiş CD, Yaşar E, et al. High-strength lightweight concrete made with scoria aggregate containing

mineral admixtures. Cem Concr Res. 2003;33(10): 1595–1599. doi: 10.1016/S0008-8846(03)00131-5.
[16] Narayanan N, Ramamurthy K. Structure and properties of aerated concrete: a review. Cem Concr Compos. 2000; 22(5):321–329. doi: 10.1016/S0958-9465(00)00016-0.
[17] Kan A, Demirboğa R. A novel material for lightweight concrete production. Cem Concr Compos. 2009;31(7): 489–495. doi: 10.1016/j.cemconcomp.2009.05.002.
[18] Jelle BP. Traditional, state-of-the-art and future thermal building insulation materials and solutions – properties, requirements and possibilities. Energy Build. 2011; 43(10):2549–2563. doi: 10.1016/j.enbuild.2011.05.015.
[19] Adhikary SK, Rudžionis Ž, Vaičiukynienė D. Development of flowable ultra-lightweight concrete using expanded glass aggregate, silica aerogel, and pre-fabricated plastic bubbles. J Build Eng. 2020;31: 101399. doi: 10.1016/j.jobe.2020.101399.
[20] Zaid O, Alsharari F, Althoey F, et al. Assessing the performance of palm oil fuel ash and lytag on the development of ultra-high-performance self-compacting lightweight concrete with waste tire steel fibers. J Build Eng. 2023;76:107112. doi: 10.1016/j.jobe.2023.107112.
[21] Calleri C, Astolfi A, Shtrepi L, et al. Characterization of the sound insulation properties of a two-layers light-weight concrete innovative façade. Appl Acoust. 2019; 145:267–277. doi: 10.1016/j.apacoust.2018.10.003.
[22] Chu H, Qin J, Gao L, et al. Effects of graphene oxide on mechanical properties and microstructure of ultra-high-performance lightweight concrete. J Sustain Cem Mater. 2023;12(6):647–660. doi: 10.1080/21650373.2022.2104757.
[23] Mahato J, Yang J, Lee N, et al. Incorporation of a high volume of cenosphere particles in low water-to-cement matrix for developing high strength and lightweight cementitious composites. J Sustain Cem Mater. 2023; 12(5):580–591. doi: 10.1080/21650373.2022.2095678.
[24] Farina I, Moccia I, Salzano C, et al. Compressive and thermal properties of non-structural lightweight concrete containing industrial byproduct aggregates. Materials (Basel). 2022;15(11):4029. doi: 10.3390/ma15114029.
[25] Saleh AN, Attar AA, Ahmed OK, et al. Improving the thermal insulation and mechanical properties of concrete using nano-SiO_2. Results Eng. 2021;12:100303. doi: 10.1016/j.rineng.2021.100303.
[26] Wang Z, Wu K, Liu S, et al. Correlation between microstructure characteristics and macroscopic behaviors of alkali residue-based foamed concrete. J Sustain Cem Mater. 2023;0:1–16. doi: 10.1080/21650373.2023.2261061.
[27] Ferenc Kristály Roland Szabó FMÁD, Mucsi G. Lightweight composite from fly ash geopolymer and glass foam. J Sustain Cem Mater. 2021;10:1–22.
[28] Kwek SY, Awang H. Utilization of industrial waste materials for the production of lightweight aggregates: a review. J Sustain Cem Mater. 2021;10(6):353–381. doi: 10.1080/21650373.2021.1891583.
[29] Gou H, Sofi M, Özyurt N, et al. Effect of pre-saturated lightweight sand on material properties of eco-friendly lightweight cementitious composites. J Sustain Cem Mater. 2023;12(5):561–579. doi: 10.1080/21650373.2022.2095677
[30] Johnson Alengaram U, Al Muhit BA, bin Jumaat MZ, et al. A comparison of the thermal conductivity of oil palm shell foamed concrete with conventional materials. Mater Des. 2013;51:522–529. doi: 10.1016/j.matdes.2013.04.078.
[31] Yu R, van Onna DV, Spiesz P, et al. Development of Ultra-Lightweight fibre reinforced concrete applying expanded waste glass. J Clean Prod. 2016;112:690–701. doi: 10.1016/j.jclepro.2015.07.082.
[32] Wang X, Wu D, Hou D, et al. The unification of light weight and ultra-high strength in LWC: a new homogeneity enhancement approach. Constr Build Mater. 2022; 315:125647. doi: 10.1016/j.conbuildmat.2021.125647.
[33] Fan D, Tian W, Yu R. Incorporation of liquid phase into solid particle packing model for precise design of low water/binder cement-based composites (LW/B-CC): modelling and experiments. Compos Part B Eng. 2022;242:110070. doi: 10.1016/j.compositesb.2022.110070.
[34] Cuce E, Cuce PM, Wood CJ, et al. Toward aerogel based thermal superinsulation in buildings: a comprehensive review. Renew Sustain Energy Rev. 2014;34: 273–299. doi: 10.1016/j.rser.2014.03.017.
[35] Dai Y-J, Tang Y-Q, Fang W-Z, et al. A theoretical model for the effective thermal conductivity of silica aerogel composites. Appl Therm Eng. 2018;128:1634–1645. doi: 10.1016/j.applthermaleng.2017.09.010.
[36] Kim S, Seo J, Cha J, et al. Chemical retreating for gel-typed aerogel and insulation performance of cement containing aerogel. Constr Build Mater. 2013;40:501–505. doi: 10.1016/j.conbuildmat.2012.11.046.
[37] Nosrati RH, Berardi U. Hygrothermal characteristics of aerogel-enhanced insulating materials under different humidity and temperature conditions. Energy Build. 2018;158:698–711. doi: 10.1016/j.enbuild.2017.09.079.
[38] Ng S, Jelle BP, Sandberg LIC, et al. Experimental investigations of aerogel-incorporated ultra-high performance concrete. Constr Build Mater. 2015;77:307–316. doi: 10.1016/j.conbuildmat.2014.12.064.
[39] Fickler S, Milow B, Ratke L, et al. Development of high performance aerogel concrete. Energy Proc. 2015; 78:406–411. doi: 10.1016/j.egypro.2015.11.684.
[40] ASTM C143/C143M-15a. 2015. Standard test method for slump of hydraulic-cement concrete, ASTM International.
[41] ASTM C39/C39M-17. A-C. 2017. Standard test method for compressive strength of cylindrical concrete specimens. ASTM International, West Conshohocken.
[42] Rashid K, Tariq S, Shaukat W. Attribution of molasses dosage on fresh and hardened performance of recycled aggregate concrete. Constr Build Mater. 2019;197:497–505. doi: 10.1016/j.conbuildmat.2018.11.249.
[43] C518 A. 2021. Standard test method for steady-state thermal transmission properties by means of the heat flow meter apparatus.
[44] ASTM C157-75. Standard test method for length change of hardened cement mortar and concrete.
[45] Liu J, Shi C, Farzadnia N, et al. Effects of pretreated fine lightweight aggregate on shrinkage and pore structure of ultra-high strength concrete. Constr Build Mater. 2019;204:276–287. doi: 10.1016/j.conbuildmat.2019.01.205.
[46] Luan C, Wang J, Gao J, et al. Changes in fractal dimension and durability of ultra-high performance concrete (UHPC) with silica fume content. ArchivCivMechEng. 2022;22(3):123. doi: 10.1007/s43452-022-00443-3.
[47] Lee NK, Koh KT, Park SH, et al. Microstructural investigation of calcium aluminate cement-based ultra-high performance concrete (UHPC) exposed to high temperatures. Cem Concr Res. 2017;102:109–118. doi: 10.1016/j.cemconres.2017.09.004.
[48] Althoey F, Zaid O, Alsulamy S, et al. Determining engineering properties of ultra-high-performance fiber-reinforced geopolymer concrete modified with different waste materials. PLoS One. 2023;18(5):e0285692. doi: 10.1371/journal.pone.0285692.
[49] Piasta J, Sawicz Z, Rudzinski L. Changes in the structure of hardened cement paste due to high temperature.

Mat Constr. 1984;17(4):291–296. doi: 10.1007/BF02479085.
[50] Shui Z, Xuan D, Chen W, et al. Cementitious characteristics of hydrated cement paste subjected to various dehydration temperatures. Constr Build Mater. 2009;23(1):531–537. doi: 10.1016/j.conbuildmat.2007.10.016.
[51] Wang J, Mu M, Liu Y. Recycled cement. Constr Build Mater. 2018;190:1124–1132. doi: 10.1016/j.conbuildmat.2018.09.181.
[52] Shaaban IG, Shaheen YB, Elsayed EL, et al. Flexural characteristics of lightweight ferrocement beams with various types of core materials and mesh reinforcement. Constr Build Mater. 2018;171:802–816. doi: 10.1016/j.conbuildmat.2018.03.167.
[53] Althoey F, Zaid O, Alsulamy S, et al. Experimental study on the properties of ultra-high-strength geopolymer concrete with polypropylene fibers and nano-silica. PLoS One. 2023;18(4):e0282435. doi: 10.1371/journal.pone.0282435.
[54] Ali M, Li X, Chouw N. Experimental investigations on bond strength between coconut fibre and concrete. Mater Des. 2013;44:596–605. doi: 10.1016/j.matdes.2012.08.038.
[55] Ho LS, Huynh T-P. Long-term mechanical properties and durability of high-strength concrete containing high-volume local fly ash as a partial cement substitution. Results Eng. 2023;18:101113. doi: 10.1016/j.rineng.2023.101113.
[56] Hematibahar M, Hasanzadeh A, Vatin NI, et al. Influence of 3D-printed reinforcement on the mechanical and fracture characteristics of ultra high performance concrete. Results Eng. 2023;19:101365. doi: 10.1016/j.rineng.2023.101365.
[57] Hosen MA, Shammas MI, Shill SK, et al. Investigation of structural characteristics of palm oil clinker based high-strength lightweight concrete comprising steel fibers. J Mater Res Technol. 2021;15:6736–6746. doi: 10.1016/j.jmrt.2021.11.105.
[58] Huang Z, Padmaja K, Li S, et al. Mechanical properties and microstructure of ultra-lightweight cement composites with fly ash cenospheres after exposure to high temperatures. Constr Build Mater. 2018;164:760–774. doi: 10.1016/j.conbuildmat.2018.01.009.
[59] Shafigh P, Muda ZC, Beddu S, et al. Thermo-mechanical efficiency of fibre-reinforced structural lightweight aggregate concrete. J Build Eng. 2022;60:105111. doi: 10.1016/j.jobe.2022.105111.
[60] Ozawa M, Uchida S, Kamada T, et al. Study of mechanisms of explosive spalling in high-strength concrete at high temperatures using acoustic emission. Constr Build Mater. 2012;37:621–628. doi: 10.1016/j.conbuildmat.2012.06.070.
[61] Prem PR, Murthy AR, Verma M. Theoretical modelling and acoustic emission monitoring of RC beams strengthened with UHPC. Constr Build Mater. 2018;158:670–682. doi: 10.1016/j.conbuildmat.2017.10.063.
[62] Xiaobao ZUO, Wei S. Full process analysis of damage and failure of concrete subjected to external sulfate attack. Kuei Suan Jen Hsueh Pao/J Chinese Ceram Soc. 2009;37.
[63] Meng C, Li W, Cai L, et al. Experimental research on durability of high-performance synthetic fibers reinforced concrete: resistance to sulfate attack and freezing-thawing. Constr Build Mater. 2020;262:120055. doi: 10.1016/j.conbuildmat.2020.120055.
[64] Liu P, Chen Y, Yu Z, et al. Evolution of the dynamic properties of concrete in a sulfate environment. Constr Build Mater. 2020;245:118468. doi: 10.1016/j.conbuildmat.2020.118468.
[65] Yang L, Fulin Y, Gaozhan Z. Synergistic effects of sustained loading and sulfate attack on the damage of UHPC based on lightweight aggregate. Constr Build Mater. 2023;374:130929. doi: 10.1016/j.conbuildmat.2023.130929.
[66] Aslam M, Shafigh P, Jumaat MZ. Drying shrinkage behaviour of structural lightweight aggregate concrete containing blended oil palm bio-products. J Clean Prod. 2016;127:183–194. doi: 10.1016/j.jclepro.2016.03.165.
[67] Feng S, Lyu J, Xiao H, et al. Application of cellulose fibre in ultra-high-performance concrete to mitigate autogenous shrinkage. J Sustain Cem Mater. 2023;12(7):842–855. doi: 10.1080/21650373.2022.2119618.
[68] Zhuang Y, Zheng D, Ng Z, et al. Effect of lightweight aggregate type on early-age autogenous shrinkage of concrete. Constr Build Mater. 2016;120:373–381. doi: 10.1016/j.conbuildmat.2016.05.105.
[69] Karaki A, Mohammad M, Masad E, et al. Theoretical and computational modeling of thermal properties of lightweight concrete. Case Stud Therm Eng. 2021;28:101683. doi: 10.1016/j.csite.2021.101683.
[70] Li X, Bao Y, Wu L, et al. Thermal and mechanical properties of high-performance fiber-reinforced cementitious composites after exposure to high temperatures. Constr Build Mater. 2017;157:829–838. doi: 10.1016/j.conbuildmat.2017.09.125.
[71] Ng S-C, Low K-S. Thermal conductivity of newspaper sandwiched aerated lightweight concrete panel. Energy Build. 2010;42(12):2452–2456. doi: 10.1016/j.enbuild.2010.08.026.
[72] Zaid O, Ahmad J, Siddique MS, et al. Effect of incorporation of rice husk ash instead of cement on the performance of steel fibers reinforced concrete. Front Mater. 2021;8:14–28. doi: 10.3389/fmats.2021.665625.
[73] Althoey F, Zaid O, Majdi A, et al. Effect of fly ash and waste glass powder as a fractional substitute on the performance of natural fibers reinforced concrete. Ain Shams Eng J. 2023;102247:102247. doi: 10.1016/j.asej.2023.102247.
[74] Zaid O, Ahmad J, Siddique MS, et al. A step towards sustainable glass fiber reinforced concrete utilizing silica fume and waste coconut shell aggregate. Sci Rep. 2021;11(1):12822. doi: 10.1038/s41598-021-92228-6.
[75] Aslam F, Zaid O, Althoey F, et al. Evaluating the influence of fly ash and waste glass on the characteristics of coconut fibers reinforced concrete. Struct Concr. 2023;24(2):2440–2459. doi: 10.1002/suco.202200183.
[76] Luan C, Wang J, Zhou Z. Synergic effect of triethanolamine and C-S-H seeding on early hydration of the limestone calcined clay cement in UHPC. Constr Build Mater. 2023;400:132675. doi: 10.1016/j.conbuildmat.2023.132675.
[77] Luan C, Wu Z, Han Z, et al. The effects of calcium content of fly ash on hydration and microstructure of ultra-high performance concrete (UHPC). J Clean Prod. 2023;415:137735. doi: 10.1016/j.jclepro.2023.137735.
[78] Wang J, Yang S, Sun Z, et al. Properties of alkali-activated slag and fly ash blended sea sand concrete exposed to elevated temperature. J Sustain Cem Mater. 2023;0:1–26. doi: 10.1080/21650373.2023.2266815.
[79] Zaid O, Mukhtar FM, M-García R, et al. Characteristics of high-performance steel fiber reinforced recycled aggregate concrete utilizing mineral filler. Case Stud Constr Mater. 2022;16:e00939. doi: 10.1016/j.cscm.2022.e00939.
[80] Martínez-García R, Jagadesh P, Zaid O, et al. The present state of the use of waste wood ash as an Eco-Efficient construction material: a review. Materials (Basel). 2022;15(15):5349. doi: 10.3390/ma15155349.

[81] Althoey F, Zaid O, de-Prado-Gil J, et al. Impact of sulfate activation of rice husk ash on the performance of high strength steel fiber reinforced recycled aggregate concrete. J Build Eng. 2022;54:104610. doi: 10.1016/j.jobe.2022.104610.
[82] Zaid O, Althoey F, García RM, et al. A study on the strength and durability characteristics of fiber-reinforced recycled aggregate concrete modified with supplementary cementitious material. Heliyon. 2023;9(9):e19978. doi: 10.1016/j.heliyon.2023.e19978.
[83] Liu Y, Jing R, Yan P. Improving environmental efficiency of ultra-high-performance concrete (UHPC) through appropriate application of ultrafine quartz powder. J Sustain Cem Mater. 2023;12(8):941–950. doi: 10.1080/21650373.2022.2139779.
[84] Saleh S, Li Y-L, Hamed E, et al. Workability, strength, and shrinkage of ultra-high-performance seawater, sea sand concrete with different OPC replacement ratios. J Sustain Cem Mater. 2023;12(3):271–291. doi: 10.1080/21650373.2022.2050831.